PAPER • OPEN ACCESS

Inversion of α-sine and α-cosine transforms on $\mathbb{R}$

To cite this article: Ly Viet Hoang and Evgeny Spodarev 2021 *Inverse Problems* **37** 085008

View the article online for updates and enhancements.

Inversion of α-sine and α-cosine transforms on $\mathbb{R}$

Ly Viet Hoang[*] and Evgeny Spodarev

Institute of Stochastics, Ulm University, Helmholtzstraße 18, 89069 Ulm, Germany

E-mail: ly.hoang@uni-ulm.de and evgeny.spodarev@uni-ulm.de

Abstract

We consider the α-sine transform of the form $T_\alpha f(y) = \int_0^\infty |\sin(xy)|^\alpha f(x)\mathrm{d}x$ for $\alpha > -1$, where f is an integrable function on $\mathbb{R}_+$. First, the inversion of this transform for $\alpha > 1$ is discussed in the context of a more general family of integral transforms on the space of weighted, square-integrable functions on the positive real line. In an alternative approach, we show that the α-sine transform of a function f admits a series representation for all $\alpha > -1$, which involves the Fourier transform of f and coefficients which can all be explicitly computed with the Gauss hypergeometric theorem. Based on this series representation we construct a system of linear equations whose solution is an approximation of the Fourier transform of f at equidistant points. Sampling theory and Fourier inversion allow us to compute an estimate of f from its α-sine transform. The same approach can be extended to a similar α-cosine transform on $\mathbb{R}_+$ for $\alpha > -1$, and the two-dimensional spherical α-sine and cosine transforms for $\alpha > -1,\ \alpha \neq 0, 2, 4, \dots$. In an extensive numerical analysis, we consider a number of examples, and compare the inversion results of both methods presented.

Keywords: Fourier analysis, integral transform, sine transform, cosine transform, spherical cosine transform, hypergeometric function, stable process

(Some figures may appear in colour only in the online journal)

1. Introduction

Spherical α-sine and α-cosine integral transforms and their inversion are of particular interest in stochastic geometry and tomography. For example when analyzing the structure of a fibrous

---

material, the so-called rose of intersections is the spherical cosine transform of the directional distribution measure of the fibers [7, 15, 23]. In the context of convex geometry, the support function of a zonoid is the α-cosine transform of some generating signed measure [24].

Spherical α-sine and α-cosine transforms, and in particular the closely related spherical Radon transform, were extensively studied in the last few decades. Groemer [11] and Helgason [12] presented many results in the fields of integral geometry and convex analysis. Further important work was done by Goodey and Weil [8, 9], Mecke [16], as well as Rubin [19, 20] in light of fiber processes and stochastic geometry.

In this paper, contrary to the spherical transforms above, we consider the integral transforms on the positive real line. We study the solution of the integral equation

$$g(y) = \int\limits_0^\infty |\sin(xy)|^\alpha f(x)\mathrm{d}x, \quad y > 0,$$

for $\alpha > -1$, where the integral transform on the right-hand side is the aforementioned α-sine transform.

The inversion of this α-sine transform is applicable in the context of stationary real harmonizable symmetric α-stable random processes. These processes are uniquely determined by their so-called control measure. Furthermore, the codifference function describes their dependence structure. It is a generalization of the covariance function to the α-stable case with $0 < \alpha < 2$, where second moments are infinite.

Assuming this control measure has a density function f, which we refer to as *spectral density*, with respect to the Lebesgue measure on $\mathbb{R}$, it can be shown the α-sine transform of f can be obtained from the codifference function. Estimation of the codifference function (and other parameters) as well as the subsequent inversion of the α-sine transform yield the spectral density f, cf section 5.

Another application example is given in the case when f is a 2π-periodic functions on $\mathbb{R}$. Then, it suffices to consider the above α-sine transform (or α-cosine transform when the integral kernel is replaced by the cosine function) on the interval $[-\pi, \pi]$. This coincides with the two-dimensional spherical α-sine and α-cosine transforms on the unit circle.

We will first introduce necessary notation and transformations in section 2. In section 3 we consider the inversion for $\alpha > 1$ in the context of a more general class of integral transformations on the space of weighted L^2-functions. We will refer to this as the *direct approach*. An alternative, approximative approach, applicable to $\alpha > -1$ is given in section 4. This approach relies on the relation between the α-sine transform and the classical Fourier transform, hence the name *Fourier approximation approach*. Our approach can also be extended to α-cosine transforms, which will be introduced later. Applications in the context of harmonizable symmetric α-stable stochastic processes and two-dimensional spherical α-sine and cosine transforms are outlined in section 5. Lastly, numerical results of each approach are presented and discussed in section 6.

2. Preliminaries

Denote by $\mathbb{R}_+$ the positive reals. Let $C^k(\mathbb{R}_+)$ be the space of k-times continuously differentiable functions on $\mathbb{R}_+$ with $C(\mathbb{R}_+)$ being the class of all continuous functions. Denote by $C_b(A)$ the space of bounded continuous functions on the interval $A \subseteq \mathbb{R}_+$. We define the space of p-integrable functions on $\mathbb{R}_+$ with respect to the measure w by $L^p(\mathbb{R}_+, w)$. Furthermore, we write $L^p(\mathbb{R}_+) = L^p(\mathbb{R}_+, \mathrm{d}x)$ for the space of p-integrable functions with respect to the Lebesgue

measure on $\mathbb{R}_+$ with L^p-norm $\|f\|_p = \left(\int_0^\infty |f(x)|^p \mathrm{d}x\right)^{1/p}$ for $f \in L^p(\mathbb{R}_+)$, $p \geqslant 1$. For $p = \infty$ this is the uniform norm $\|f\|_\infty = \mathrm{ess\,sup}_{x \in \mathbb{R}_+} |f(x)|$. We say that a sequence $(f_n)_{n \in \mathbb{N}}$ converges to some limit f in L^p if the L^p-distance $\|f_n - f\|_p$ converges to 0 as n tends to infinity.

Define the α-*sine transform* T_α for $\alpha > -1$ by

$$T_\alpha f(y) = \int\limits_0^\infty |\sin(xy)|^\alpha f(x)\mathrm{d}x, \tag{1}$$

which is even in its argument, therefore, it suffices to consider $y \in \mathbb{R}_+$.

We define the weighted function space $L^1_{w,\alpha}(\mathbb{R}_+)$ by

$$L^1_{w,\alpha}(\mathbb{R}_+) = \begin{cases} L^1(\mathbb{R}_+), & \alpha \geqslant 0, \\[2mm] L^1(\mathbb{R}_+) \cap L^1\left(\mathbb{R}_+, \max\left\{\dfrac{1}{x}, 1\right\}\mathrm{d}x\right), & -1 < \alpha < 0. \end{cases} \tag{2}$$

Lemma 1. *For any $f \in L^1_{w,\alpha}(\mathbb{R}_+)$ the function $T_\alpha f$ is well defined almost everywhere on $\mathbb{R}_+$. Additionally, it holds that $T_\alpha f(0) = 0$ in case $\alpha > 0$.*

Proof. Let $\alpha \geqslant 0$. Note that by the triangle inequality it holds that $|T_\alpha f(y)| \leqslant T_\alpha |f|(y) \leqslant \|f\|_1$ for all $y \in \mathbb{R}_+$. The relation $T\alpha f(0) = 0$ is trivially satisfied for $\alpha > 0$. For $-1 < \alpha < 0$ the finiteness of $\int_0^K |T_\alpha f(y)|\mathrm{d}y$ would imply that $T_\alpha f$ is finite almost everywhere on the interval $[0, K]$. Again, by the triangle inequality it holds that

$$\int\limits_0^K |T_\alpha f(y)|\mathrm{d}y \leqslant \int\limits_0^K T_\alpha |f|(y)\mathrm{d}y = \int\limits_0^K \left(\int\limits_0^\infty |\sin(xy)|^\alpha |f(x)|\mathrm{d}x\right)\mathrm{d}y.$$

Using Fubini's theorem we can further compute

$$\int\limits_0^K \left(\int\limits_0^\infty |\sin(xy)|^\alpha |f(x)|\mathrm{d}x\right)\mathrm{d}y = \int\limits_0^\infty \left(\int\limits_0^K |\sin(xy)|^\alpha \mathrm{d}y\right) |f(x)|\mathrm{d}x$$

$$= \int\limits_0^\infty \left(\frac{1}{x}\int\limits_0^{Kx} |\sin(u)|^\alpha \mathrm{d}u\right) |f(x)|\mathrm{d}x,$$

where the last equality stems from the substitution $u = xy$. Since $|\sin(u)|$ is π-periodic, we can estimate

$$\frac{1}{x}\int\limits_0^{Kx} |\sin(u)|^\alpha \mathrm{d}u \leqslant \frac{1}{x}\left(\left\lfloor\frac{Kx}{\pi}\right\rfloor + 1\right) \underbrace{\int\limits_0^\pi |\sin(u)|^\alpha \mathrm{d}u}_{=:C_\alpha}$$

$$\leqslant \frac{1}{x}\left(\frac{Kx}{\pi} + 1\right) C_\alpha = \left(\frac{K}{\pi} + \frac{1}{x}\right) C_\alpha,$$

where the constant C_α is given by $C_\alpha = \sqrt{\pi} \frac{\Gamma\left(\frac{1+\alpha}{2}\right)}{\Gamma\left(1+\frac{\alpha}{2}\right)}$ for $\alpha > -1$. The above converges to K/π as $x \to \infty$, and demanding $f \in L^1(\mathbb{R}_+) \cap L^1\left(\mathbb{R}_+, \max\left\{\frac{1}{x}, 1\right\} dx\right)$ ensures that $\int_0^K |T_\alpha f(y)| dy < \infty$. Hence, by the integrability of $T_\alpha f$ on $[0, K]$, it holds that $|T_\alpha f|$ is finite almost everywhere on $[0, K]$. Using the subadditivity of the Lebesgue measure, it follows that $T_\alpha f$ is finite almost everywhere on $\mathbb{R}_+$, i.e.

$$\mathcal{L}\left(\{y \in \mathbb{R}_+ : |T_\alpha f(y)| = \infty\}\right) = \mathcal{L}\left(\bigcup_{K \in \mathbb{N}} \{y \in [0, K] : |T_\alpha f(y)| = \infty\}\right)$$

$$\leqslant \sum_{K \in \mathbb{N}} \underbrace{\mathcal{L}\left(\{y \in [0, K] : |T_\alpha f(y)| = \infty\}\right)}_{=0,\ K \in \mathbb{N}} = 0,$$

where $\mathcal{L}$ denotes the Lebesgue measure. $\qquad\square$

For $\alpha \geqslant 0$, using the triangle inequality for integrals, one can show that the transform T_α is a bounded linear operator from $L^1_{w,\alpha}$ into the space of bounded continuous functions on $\mathbb{R}_+$. In the case $-1 < \alpha < 0$, one needs to impose more conditions on the function f such that T_α is bounded. Both cases are analyzed in detail in theorem 3.

The goal is to invert the transform T_α, or in other words to solve the integral equation $g = T_\alpha f$ for the function f. Each approach, presented in sections 3 and 4, respectively, requires the introduction of different integral operators and special functions, which will be given in the following.

Section 4 establishes the close relationship between the α-sine transform (1) and the *classical Fourier transform* on $\mathbb{R}$. The α-sine transform is well defined for all functions from the space $L^1_{w,\alpha}(\mathbb{R}_+)$. We can evenly extend functions $f \in L^1_{w,\alpha}(\mathbb{R}_+)$ to the negative half of the real line by setting $f(-x) = f(x)$ for all $x \in \mathbb{R}$. For ease of notation, we denote this by $f \in L^1_{e,w,\alpha}(\mathbb{R}_+)$. Similarly, we denote by $L^p_e(\mathbb{R})$ the space of all even L^p-functions.

Define the *Fourier transform* and its *inverse transform* on the space of integrable functions $L^1(\mathbb{R})$ by

$$\mathcal{F}v(y) = \int_{\mathbb{R}} e^{ixy} v(x) dx, \qquad \mathcal{F}^{-1}w(x) = \frac{1}{2\pi} \int_{\mathbb{R}} e^{-ixy} w(y) dy,$$

for $v, w \in L^1(\mathbb{R})$. By the Euler formula, the integral kernels e^{ixy} and e^{-ixy} in the definition of the Fourier transform above can be replaced by $\cos(xy)$ for even functions $v, w \in L^1_e(\mathbb{R})$.

Note that on the space of Lebesgue integrable functions $L^1(\mathbb{R})$ the above Fourier transform is bounded, uniformly continuous, and vanishes at infinity by the Riemann–Lebesgue lemma [10, proposition 2.2.17]. It is well known that the Fourier transform of an integrable function might not be integrable itself. Therefore, only under certain additional conditions on v the Fourier inversion theorem $v = \mathcal{F}^{-1}\mathcal{F}v = \mathcal{F}\mathcal{F}^{-1}v$ is applicable, e.g. if v is a Schwartz function, or if it is integrable and square integrable [10, section 2.2.4]. On the space $L^1(\mathbb{R}) \cap L^2(\mathbb{R})$ the Fourier transform $\mathcal{F}$ is a L^2-isometry, i.e. $\|\mathcal{F}v\|_2 = 2\pi\|v\|_2$ by the Plancherel theorem. Furthermore, let $(v_n)_{n \in \mathbb{N}}$ be a sequence of functions in $L^1(\mathbb{R}) \cap L^2(\mathbb{R})$ with $v_n \to v$ in L^2-norm as $n \to \infty$. Then, the convergence is preserved under the Fourier transform in the sense that $\mathcal{F}v_n \to \mathcal{F}v$ in the L^2-norm as $n \to \infty$ [10, equation 2.2.16].

For section 3 we consider the *Fourier transform and its inverse transform on the multiplicative group* $(\mathbb{R}_+, \cdot)$ by $\mathcal{F}_+ : L^2\left(\mathbb{R}_+, \frac{dx}{x}\right) \to L^2\left(\mathbb{R}_+, \frac{dx}{x}\right)$ with

$$\mathcal{F}_+ v(y) = \int_0^\infty e^{-i\log(x)\log(y)} v(x) \frac{dx}{x},$$

$$\mathcal{F}_+^{-1} w(x) = \frac{1}{2\pi} \int_0^\infty e^{i\log(x)\log(y)} w(y) \frac{dy}{y}$$

for $v, w \in L^2\left(\mathbb{R}_+, \frac{dx}{x}\right)$, as well as the similarity transform $\mathcal{M} : L^2\left(\mathbb{R}_+, x^c\, dx\right) \to L^2\left(\mathbb{R}_+, \frac{dx}{x}\right)$ and its inverse by

$$\mathcal{M}v(y) = y^{(c+1)/2} v(y), \qquad \mathcal{M}^{-1} w(x) = x^{-(c+1)/2} w(x)$$

for $v \in L^2\left(\mathbb{R}_+, x^c\, dx\right)$, $w \in L^2\left(\mathbb{R}_+, \frac{dx}{x}\right)$.

Additionally, we state the following useful result. For any complex number $z \in \mathbb{C}$ one can expand

$$(1 + x)^z = \sum_{k=0}^\infty \binom{z}{k} x^k, \tag{3}$$

where $\binom{z}{k}$ is the *generalized binomial coefficient* defined by

$$\binom{z}{k} = \frac{\Gamma(z+1)}{\Gamma(z-k+1)\Gamma(k+1)} = \frac{z(z-1)\dots(z-k+1)}{k!}.$$

Here, Γ denotes the gamma function. For $|x| < 1$ the series converges absolutely for any $z \in \mathbb{C}$. If $|x| = 1$ absolute convergence is given if and only if $\mathrm{Re}(z) > 0$, for $-1 < \mathrm{Re}(z) \leqslant 0$ the series converges if $x \neq -1$.

Lastly, the so-called *generalized hypergeometric function* $_pF_q$ and the special *Gauss hypergeometric function* $_2F_1$, which are well known in mathematical physics, play important roles in the Fourier approximation approach.

The generalized hypergeometric function $_pF_q$ with $p, q \in \mathbb{N}_0$ is defined by

$$_pF_q\left[a_1, \dots, a_p; b_1, \dots, b_q; z\right] = \sum_{k=0}^\infty \frac{(a_1)_k \dots (a_p)_k}{(b_1)_k \dots (b_q)_k} \frac{z^k}{k!} \tag{4}$$

for any complex numbers $a_1, \dots, a_p, b_1, \dots, b_q \in \mathbb{C}$ and $z \in \mathbb{C}$, where $(\cdot)_n$ is called the *Pochhammer symbol*, or *rising factorial*, with

$$(a)_n = \begin{cases} 1, & n = 0, \\ a(a+1)(a+2)\dots(a+n-1), & n \geqslant 1. \end{cases}$$

For $p \leqslant q$ the generalized hypergeometric function converges for all $z \in \mathbb{C}$, and for $p > q+1$ only if $z = 0$. In the case $p = q+1$ the series converges if $|z| < 1$, and when $z = 1$ provided $\mathrm{Re}\left(\sum b_i - \sum a_i\right) > 0$ or when $z = -1$ provided $\mathrm{Re}\left(\sum b_i - \sum a_i + 1\right) > 0$ [1, p 8].

For the Gauss hypergeometric function $_2F_1$ it holds that

$$_2F_1[a, b; c; z] = \sum_{k=0}^\infty \frac{(a)_k (b)_k}{(c)_k} \frac{z^k}{k!}$$

for $a, b, c, z \in \mathbb{C}$, and for $z = 1$ provided $\mathrm{Re}(c - a - b) > 0$ the series converges absolutely with

$$_2F_1[a, b; c; 1] = \sum_{k=0}^{\infty} \frac{(a)_k(b)_k}{c_k} \frac{1}{k!} = \frac{\Gamma(c)\Gamma(c - a - b)}{\Gamma(c - a)\Gamma(c - b)}. \tag{5}$$

This classical result is known as the Gauss hypergeometric theorem [1, section 1.3].

3. Direct approach for $\alpha > 1$

In [6] the existence and uniqueness of a solution to integral equations of the form

$$w(y) = \int_{\mathrm{supp}(\gamma)} \beta(t) v\left(\gamma(t)y\right) \mathrm{d}t$$

for given measurable functions $\beta, \gamma : \mathbb{R}^d \to \mathbb{R}$, and a weighted L^2-function v on $\mathbb{R}$ is analyzed. The set $\mathrm{supp}(\gamma) = \left\{ t \in \mathbb{R}^d : \gamma(t) \neq 0 \right\}$ denotes the support of γ. Their solution theory is based on operators on the multiplicative group on $\mathbb{R}^{\times} = \mathbb{R} \backslash \{0\}$. Since even functions are of interest, it suffices to consider the positive reals $\mathbb{R}_+$ only.

Define the linear integral operator $\mathcal{G} : L^2\left(\mathbb{R}_+, x^c \, \mathrm{d}x\right) \to L^2\left(\mathbb{R}_+, x^c \, \mathrm{d}x\right)$ by

$$\mathcal{G}v(y) = \int_{\mathrm{supp}(\gamma)} \beta(t) v\left(\gamma(t)y\right) \mathrm{d}t, \quad y > 0, \tag{6}$$

where the functions β and γ are chosen such that the constant

$$C = \int_{\mathrm{supp}(\gamma)} |\beta(t)| \, |\gamma(t)|^{-\frac{c+1}{2}} \mathrm{d}t < \infty \tag{7}$$

is finite. Furthermore, we introduce the function $\mu : \mathbb{R}_+ \to \mathbb{C}$ given by

$$\mu(x) = \int_{\mathrm{supp}(\gamma)} \beta(t) |\gamma(t)|^{-\frac{c+1}{2}} \mathrm{e}^{\mathrm{i} \log(x) \log |\gamma(t)|} \mathrm{d}t. \tag{8}$$

The function μ is bounded and its continuity follows from Lebesgue's dominated convergence theorem.

The following lemma on the injectivity and surjectivity of the operator $\mathcal{G}$ can be derived from ([6, corollary 2.4]) which states the results in the context of the multiplicative group $(\mathbb{R}^{\times}, \cdot)$.

Lemma 2. *Assume that $C < \infty$, and let $\mu : \mathbb{R} \to \mathbb{C}$ be the bounded, continuous function defined in (8). Then, the operator $\mathcal{G} : L^2\left(\mathbb{R}_+, x^c \, \mathrm{d}x\right) \to L^2\left(\mathbb{R}_+, x^c \, \mathrm{d}x\right)$ as defined in (6) is*

(a) *Injective if and only if $\mu \neq 0$ almost everywhere on $\mathbb{R}_+$ (with respect to the Lebesgue measure).*
(b) *Bijective if and only if $\inf_{x \in \mathbb{R}_+} |\mu(x)| > 0$.*

It is now possible to consider the α-sine transform in the context of the integral operator $\mathcal{G}$. For all $y \in \mathbb{R}_+$, the transform $T_\alpha f$ can be reformulated by substituting $t = xy$ and setting $z = 1/y$ to

$$T_\alpha f(y) = \int_0^\infty |\sin(xy)|^\alpha f(x)\mathrm{d}x = z\int_0^\infty |\sin(t)|^\alpha f(tz)\mathrm{d}t = z\mathcal{G}_+ v(z)$$

with $\beta(t) = |\sin(t)|^\alpha$, $\gamma(t) = t$ with $\mathrm{supp}(\gamma) = \mathbb{R}_+$ and $v = f$. With $g = T_\alpha f$ this yields the equation

$$\mathcal{G}f(z) = z^{-1}g(z^{-1}) \tag{9}$$

for all $z \in \mathbb{R}_+$. Plugging in the functions β and γ into the definitions of $\mathcal{G}$ and μ, we can state the following theorem similar to [6, proposition 2.1, theorem 2.3]:

Theorem 1.   *Let $c = 1 + \delta$ with $\delta > 0$ such that $\alpha \geqslant 1 + \delta/2$. Then*

$$C = \int_0^\infty |\sin(t)|^\alpha t^{-\frac{c+1}{2}}\mathrm{d}t < \infty, \tag{10}$$

and

(a) *The linear operator $\mathcal{G} : L^2\left(\mathbb{R}_+, x^c\,\mathrm{d}x\right) \to L^2\left(\mathbb{R}_+, x^c\,\mathrm{d}x\right)$ given by*

$$\mathcal{G}v(y) = \int_0^\infty |\sin(t)|^\alpha v(ty)\mathrm{d}t, \quad y > 0, \tag{11}$$

   is bounded on $L^2\left(\mathbb{R}_+, x^c\,\mathrm{d}x\right)$ with operator norm $\|\mathcal{G}\| \leqslant C$.
(b) *For all functions $v \in L^2\left(\mathbb{R}_+, \frac{\mathrm{d}x}{x}\right)$ the equation $\tilde{\mathcal{G}}v = \mu v$ holds, where $\tilde{\mathcal{G}} = \mathcal{F}_+\mathcal{M}\mathcal{G}\mathcal{M}^{-1}\mathcal{F}_+^{-1}$ and $\mu : \mathbb{R}_+ \to \mathbb{C}$ with*

$$\mu(x) = \int_0^\infty |\sin(t)|^\alpha t^{-\frac{c+1}{2}}e^{i\log(t)\log(x)}\mathrm{d}t, \quad x > 0. \tag{12}$$

Proof.   The application of [6, proposition 2.1] yields (a). For (b) note that $\tilde{\mathcal{G}}u = \tilde{\mu}u$ holds if and only if $\tilde{\mathcal{G}}\mathcal{F}_+\mathcal{M}u = \tilde{\mu}\mathcal{F}_+\mathcal{M}u$ is true for all $u \in L^2\left(\mathbb{R}_+, \frac{\mathrm{d}x}{x}\right)$. For $y > 0$

$$\mathcal{F}_+\mathcal{M}u(y) = \int_0^\infty x^{\frac{c+1}{2}}u(x)e^{-i\log(x)\log(y)}\frac{\mathrm{d}x}{x} = \int_0^\infty x^{\frac{c-1}{2}}u(x)e^{-i\log(x)\log(y)}\mathrm{d}x,$$

and hence

$$\tilde{\mathcal{G}}\mathcal{F}_+\mathcal{M}u(y) = \mathcal{F}_+\mathcal{M}_+\mathcal{G}_+u(y) = \int_0^\infty x^{\frac{c-1}{2}}\left[\int_0^\infty |\sin(t)|^\alpha u(tx)\mathrm{d}t\right]$$

$$\times e^{-i\log(x)\log(y)}\mathrm{d}x$$

$$= \int_0^\infty \int_0^\infty s^{\frac{c-1}{2}} t^{-\frac{c-1}{2}} |\sin(t)|^\alpha u(s) e^{-i \log(s/t) \log(y)} \frac{\mathrm{d}s}{t} \, \mathrm{d}t$$

$$= \int_0^\infty |\sin(t)|^\alpha t^{-\frac{c+1}{2}} e^{i \log(t) \log(y)} \mathrm{d}t$$

$$\times \int_0^\infty s^{\frac{c-1}{2}} u(s) e^{-i \log(s) \log(y)} st = \mu(y) \mathcal{F}_+ \mathcal{M} u(y)$$

using Fubini's theorem and the substitution $x = s/t$. $\qquad\square$

We can now state an inversion formula for the operator $\mathcal{G}_+$ solving equation (9).

Corollary 1. *Let $f \in L^1\left(\mathbb{R}_+, \mathrm{d}x\right) \cap L^2\left(\mathbb{R}_+, x^c \, \mathrm{d}x\right)$, where $c = 1 + \delta$ for some $\delta > 0$ with $\alpha \geqslant 1 + \delta/2$. Assume that the function $z^{-1} g(z^{-1})$ belongs to the space $L^2\left(\mathbb{R}_+, x^c \, \mathrm{d}x\right)$. Then*

$$f(x) = \left(\mathcal{M}^{-1} \mathcal{F}_+^{-1} \frac{1}{\mu} \mathcal{F}_+ \mathcal{M} \left[z^{-1} g\left(z^{-1}\right) \right] \right)(x) \tag{13}$$

for all $x \in \mathbb{R}_+$. The operator $\mathcal{G}$ on $L^2\left(\mathbb{R}_+, x^c \, \mathrm{d}x\right)$ is injective, as $\mu \neq 0$ almost everywhere on $\mathbb{R}_+$, but not surjective since $\inf_{x>0} |\mu(x)| = 0$.

Proof. The inversion formula (13) is a direct consequence of theorem 1. It is easy to see that $\mu \neq 0$ almost everywhere on $\mathbb{R}_+$. To show that $\mathcal{G}$ is not surjective, i.e. $\inf_{x>0} |\mu(x)| = 0$, note that $1 < \frac{c+1}{2} \leqslant \alpha$ holds, and one can compute

$$|\mu(x)| = \left| \int_0^\infty |\sin(t)|^\alpha t^{-\frac{c+1}{2}} e^{i \log(t) \log(x)} \mathrm{d}t \right| \leqslant \left| \int_0^1 |\sin(t)|^\alpha t^{-\frac{c+1}{2} + i \log(x)} \mathrm{d}t \right|$$

$$+ \left| \int_1^\infty |\sin(t)|^\alpha t^{-\frac{c+1}{2} + i \log(x)} \mathrm{d}t \right|$$

$$\leqslant \left| \int_0^1 t^{\alpha - \frac{c+1}{2} + i \log(x)} \mathrm{d}t \right| + \left| \int_1^\infty t^{-\frac{c+1}{2} + i \log(x)} \mathrm{d}t \right|$$

$$= \frac{1}{\left| \alpha - \frac{c+1}{2} + 1 + i \log(x) \right|} + \frac{1}{\left| \frac{c+1}{2} - 1 - i \log(x) \right|} \to 0$$

as $x \to \infty$. $\qquad\square$

Corollary 1 gives an inversion formula which computes the solution of the integral equation $g = Tf$ directly. We will later see though that the involved operators $\mathcal{F}_+$, $\mathcal{M}$ and the function μ are numerically unstable, and inversion results are rather unsatisfying in practice. An even more significant drawback is the restriction to $\alpha > 1$. The numerical analysis of the direct approach can be found in section 6.1.

4. Fourier approximation approach

Recall the space $L^1_{w,\alpha}(\mathbb{R}_+)$ defined in the preliminaries by

$$
L^1_{w,\alpha}(\mathbb{R}_+) = \begin{cases} L^1(\mathbb{R}_+), & \alpha \geqslant 0, \\ L^1(\mathbb{R}_+) \cap L^1\left(\mathbb{R}_+, \max\left\{\dfrac{1}{x}, 1\right\} \mathrm{d}x\right), & -1 < \alpha < 0. \end{cases}
$$

Remark 1. In the following, the even extension of $f \in L^1_{w,\alpha}(\mathbb{R}_+)$ to the whole real line is also denoted by f, whenever we consider the Fourier transform $\mathcal{F}f$.

Consider the transform $T_2 f(y) = \int_0^\infty |\sin(xy)|^2 f(x)\mathrm{d}x$. Applying the cosine double angle formula $\cos(2x) = 1-2\sin^2(x)$ yields

$$
T_2 f(y) = \frac{\mathcal{F}f(0)}{4} - \frac{\mathcal{F}f(2y)}{4}.
$$

Assuming the constant $\mathcal{F}f(0)$ is known, the inversion of T_2 is simply achieved by applying the Fourier inverse transform to $\mathcal{F}f(0) - 2T_2 f$. But for $\alpha > -1, \alpha \neq 2$, the cosine double angle formula alone does not help a lot.

In following section, we first prove a series representation of T_α. Section 4.2 then establishes the Fourier approximation approach, where the Fourier transform $\mathcal{F}f$ is approximated from the transform $T_\alpha f$. Lastly, section 4.3 presents an interpolation method from which the function f is computed.

4.1. Series representation

Theorem 2.

(a) Let $\alpha > -1$. The function $\frac{1}{2}\left|\sin\left(\frac{x}{2}\right)\right|^\alpha$ admits the Fourier series expansion

$$
\frac{1}{2}\left|\sin\left(\frac{x}{2}\right)\right|^\alpha = \frac{c_0}{2} + \sum_{j=1}^\infty c_j \cos(jx)
$$

with real Fourier coefficients

$$
c_j = \begin{cases} \dfrac{(-1)^j}{2^\alpha} \dfrac{\Gamma(1+\alpha)}{\Gamma\left(\frac{\alpha}{2}-j+1\right)\Gamma\left(\frac{\alpha}{2}+j+1\right)}, & \alpha \neq 2k, \ j \in \mathbb{N}_0, \\ \dfrac{(-1)^j}{4^k} \begin{pmatrix} 2k \\ k-j \end{pmatrix}, & \alpha = 2k, \ j = 0,\dots,k, \ k \in \mathbb{N}_0, \\ 0, & \alpha = 2k, \ j > k, \ k \in \mathbb{N}_0. \end{cases} \quad (14)
$$

The Fourier series converges absolutely and uniformly on $\mathbb{R}$ for $\alpha \geqslant 0$. It converges almost everywhere on $\mathbb{R}$ for $-1 < \alpha < 0$.

(b) For any integrable function $f \in L^1_{w,\alpha}(\mathbb{R}_+)$, $\alpha > -1$, the integral transform $T_\alpha f(y) = \int_0^\infty |\sin(xy)|^\alpha f(x)\mathrm{d}x$ has the series representation

$$
T_\alpha f(y) = \frac{c_0}{2}\mathcal{F}f(0) + \sum_{j=1}^\infty c_j \mathcal{F}f(2jy). \quad (15)
$$

In the case $\alpha = 2k$, $k \in \mathbb{N}_0$, the above infinite series in expression (15) becomes a finite sum, i.e.

$$T_\alpha f(y) = \frac{c_0}{2} \mathcal{F} f(0) + c_1 \mathcal{F} f(2y) + c_2 \mathcal{F} f(4y) + \cdots + c_k \mathcal{F} f(2ky).$$

Proof.

(a) Let $\alpha > -1$. First of all, note that

$$\frac{1}{2} \left| \sin\left(\frac{x}{2}\right) \right|^\alpha = \frac{1}{2} \left(\sin^2\left(\frac{x}{2}\right) \right)^{\alpha/2} = \frac{1}{2^{\alpha/2+1}} (1 - \cos(x))^{\alpha/2}$$

$$= \frac{1}{2^{\alpha/2+1}} \sum_{k=0}^\infty \binom{\alpha/2}{k} (-1)^k \cos^k(x)$$

for all $x, y \in \mathbb{R}$ by the binomial series (3). Since $|\cos(x)| < 1$ almost everywhere on $\mathbb{R}$ the series above converges absolutely almost everywhere for any $\alpha > -1$. Splitting the series into an odd and even summands and applying the cosine power formulae

$$\cos^k(2xy) = \begin{cases} \dfrac{2}{2^{2n-1}} \displaystyle\sum_{l=0}^{n-1} \binom{2n-1}{l} \cos((2n-1-2l)2xy), & k = 2n-1, \\[4mm] \dfrac{1}{2^{2n}} \binom{2n}{n} + \dfrac{2}{2^{2n}} \displaystyle\sum_{l=0}^{n-1} \binom{2n}{l} \cos((2n-2l)2xy), & k = 2n, \end{cases} \quad n \in \mathbb{N},$$

yields

$$\frac{1}{2} \left| \sin\left(\frac{x}{2}\right) \right|^\alpha = \frac{1}{2^{\alpha/2+1}} \left(1 - \sum_{n=1}^\infty \binom{\alpha/2}{2n-1} \cos^{2n-1}(x) \right.$$

$$+ \sum_{n=1}^\infty \binom{\alpha/2}{2n} \cos^{2n}(x) \Bigg)$$

$$= \frac{1}{2^{\alpha/2+1}} \left(1 - \sum_{n=1}^\infty \binom{\alpha/2}{2n-1} \frac{2}{2^{2n-1}} \right.$$

$$\times \sum_{l=0}^{n-1} \binom{2n-1}{l} \cos((2n-1-2l)x)$$

$$+ \sum_{n=1}^\infty \binom{\alpha/2}{2n} \frac{1}{2^{2n}} \binom{2n}{n} + \sum_{n=1}^\infty \binom{\alpha/2}{2n} \frac{2}{2^{2n}}$$

$$\times \sum_{l=0}^{n-1} \binom{2n}{l} \cos((2n-2l)x) \Bigg)$$

$$= \frac{1}{2^{\alpha/2+1}} \left(\sum_{n=0}^\infty \binom{\alpha/2}{2n} \binom{2n}{n} \frac{1}{4^n} \right.$$

$$+ 2 \sum_{k=1}^\infty \binom{\alpha/2}{k} \frac{(-1)^k}{2^k} \sum_{l=0}^{\lfloor \frac{k-1}{2} \rfloor} \binom{k}{l} \cos((k-2l)x) \Bigg).$$

Substituting $j = k - 2l$ and rearranging the series above we get

$$\frac{1}{2}\left|\sin\left(\frac{x}{2}\right)\right|^\alpha = \underbrace{\frac{1}{2^{\alpha/2+1}}\sum_{n=0}^\infty \binom{\alpha/2}{2n}\binom{2n}{n}\frac{1}{4^n}}_{=:c} + \sum_{j=1}^\infty \underbrace{\left(\frac{(-1)^j}{2^{\alpha/2}}\sum_{l=0}^\infty \binom{\alpha/2}{j+2l}\binom{j+2l}{l}\frac{1}{2^{j+2l}}\right)}_{=:c_j}\cos(jx).$$

(16)

The coefficients c and c_j, $j \in \mathbb{N}$, can be expressed in terms of the Gauss hypergeometric function aforementioned in section 2.

First, we compute the constant c in equation (16). Note that

$$\binom{\alpha/2}{2n}\binom{2n}{n}\frac{1}{4^n} = \frac{\frac{\alpha}{2}\left(\frac{\alpha}{2}-1\right)\ldots\left(\frac{\alpha}{2}-2n+2\right)+\left(\frac{\alpha}{2}-2n+1\right)}{(2n)!}\frac{(2n)!}{n!n!}\frac{1}{4^n}$$

$$= \frac{-\frac{\alpha}{4}\left(-\frac{\alpha}{4}+\frac{1}{2}\right)\left(-\frac{\alpha}{4}+1\right)\left(-\frac{\alpha}{4}+\frac{3}{2}\right)\ldots\left(-\frac{\alpha}{4}+n-1\right)\left(-\frac{\alpha}{4}+\frac{1}{2}+n-1\right)}{n!}$$

$$\times \frac{(-2)^{2n}}{4^n}\frac{1}{n!}$$

$$= \frac{\left(-\frac{\alpha}{4}\right)_n\left(-\frac{\alpha}{4}+\frac{1}{2}\right)_n}{(1)_n}\frac{1}{n!}.$$

For all $\alpha > -1$ it holds that $1 - \left(-\frac{\alpha}{4}\right) - \left(-\frac{\alpha}{4}+\frac{1}{2}\right) = \frac{1}{2} + \frac{\alpha}{2} > 0$, and the Gauss hypergeometric theorem (5) yields

$$\sum_{n=0}^\infty \binom{\alpha/2}{2n}\binom{2n}{n}\frac{1}{4^n} = \sum_{n=0}^\infty \frac{\left(-\frac{\alpha}{4}\right)_n\left(-\frac{\alpha}{4}+\frac{1}{2}\right)_n}{(1)_n}\frac{1}{n!} = {}_2F_1\left[-\frac{\alpha}{4}, -\frac{\alpha}{4}+\frac{1}{2}; 1; 1\right]$$

$$= \frac{\Gamma\left(\frac{1}{2}+\frac{\alpha}{2}\right)}{\Gamma\left(1+\frac{\alpha}{4}\right)\Gamma\left(\frac{1}{2}+\frac{\alpha}{4}\right)}.$$

Hence, the constant c is given by

$$c = \frac{1}{2^{\alpha/2+1}}\sum_{n=0}^\infty \binom{\alpha/2}{2n}\binom{2n}{n}\frac{1}{4^n} = \frac{1}{2^{\alpha/2+1}}\frac{\Gamma\left(\frac{1}{2}+\frac{\alpha}{2}\right)}{\Gamma\left(1+\frac{\alpha}{4}\right)\Gamma\left(\frac{1}{2}+\frac{\alpha}{4}\right)}. \quad (17)$$

For all coefficients c_j, $j \in \mathbb{N}$, recall from equation (16)

$$c_j = \frac{(-1)^j}{2^{\alpha/2}}\sum_{n=0}^\infty \binom{\alpha/2}{j+2n}\binom{j+2n}{n}\frac{1}{2^{j+2n}}.$$

We compute

$$\binom{\alpha/2}{j+2l}\binom{j+2l}{l}\frac{1}{2^{j+2l}} = \frac{1}{2^j}\frac{\frac{\alpha}{2}\left(\frac{\alpha}{2}-1\right)\ldots\left(\frac{\alpha}{2}-j-2l+1\right)}{(j+2l)!}$$

$$\times \frac{(j+2l)!}{l!(j+l)!}\frac{1}{4^l}$$

$$= \frac{\frac{\alpha}{2}\left(\frac{\alpha}{2}-1\right)\ldots\left(\frac{\alpha}{2}-j+1\right)}{2^j\,j!}\frac{\left(\frac{\alpha}{2}-j\right)\left(\frac{\alpha}{2}-j-1\right)\ldots\left(\frac{\alpha}{2}-j-2l+1\right)}{(j+1)_l}\frac{1}{4^l}\frac{1}{l!}$$

$$= \frac{\Gamma\left(\frac{\alpha}{2}+1\right)}{2^j \Gamma\left(\frac{\alpha}{2}-j+1\right) j!} \frac{\left(-\frac{\alpha}{4}+\frac{j}{2}\right)_l \left(-\frac{\alpha}{4}+\frac{j}{2}+\frac{1}{2}\right)_l}{(j+1)_l} \frac{(-2)^{2l}}{4^l} \frac{1}{l!}$$

$$= \frac{\Gamma\left(\frac{\alpha}{2}+1\right)}{2^j \Gamma\left(\frac{\alpha}{2}-j+1\right) j!} \frac{\left(-\frac{\alpha}{4}+\frac{j}{2}\right)_l \left(-\frac{\alpha}{4}+\frac{j}{2}+\frac{1}{2}\right)_l}{(j+1)_l} \frac{1}{l!}.$$

Note that $j+1-\left(-\frac{\alpha}{4}+\frac{j}{2}\right)-\left(-\frac{\alpha}{4}+\frac{j}{2}+\frac{1}{2}\right) = \frac{1}{2}+\frac{\alpha}{2} > 0$ for all $\alpha > -1$. Applying the Gauss hypergeometric theorem (5) and Legendre's duplication formula $\Gamma\left(\frac{x}{2}\right)\Gamma\left(\frac{x+1}{2}\right) = \sqrt{\pi}/2^{x-1}\Gamma(x)$, it follows that

$$\sum_{l=0}^{\infty} \binom{\alpha/2}{j+2l}\binom{j+2l}{l}\frac{1}{2^{j+2l}} = \frac{\Gamma\left(\frac{\alpha}{2}+1\right)}{2^j \Gamma\left(\frac{\alpha}{2}-j+1\right) j!}$$

$$\times \sum_{l=0}^{\infty} \frac{\left(-\frac{\alpha}{4}+\frac{j}{2}\right)_l \left(-\frac{\alpha}{4}+\frac{j}{2}+\frac{1}{2}\right)_l}{(j+1)_l} \frac{1}{l!}$$

$$= \frac{\Gamma\left(\frac{\alpha}{2}+1\right)}{2^j \Gamma\left(\frac{\alpha}{2}-j+1\right) j!} {}_2F_1$$

$$\times \left[-\frac{\alpha}{4}+\frac{j}{2}, -\frac{\alpha}{4}+\frac{j}{2}+\frac{1}{2}; j+1; 1\right]$$

$$= \frac{\Gamma\left(\frac{\alpha}{2}+1\right)}{2^j \Gamma\left(\frac{\alpha}{2}-j+1\right) j!}$$

$$\times \frac{\Gamma(j+1)\Gamma\left(\frac{1}{2}+\frac{\alpha}{2}\right)}{\Gamma\left(1+\frac{\alpha}{4}+\frac{j}{2}\right)\Gamma\left(\frac{1}{2}+\frac{\alpha}{4}+\frac{j}{2}\right)}$$

$$= \frac{\frac{\sqrt{\pi}}{2^\alpha}\Gamma(1+\alpha)}{2^j \Gamma\left(\frac{\alpha}{2}-j+1\right) \frac{\sqrt{\pi}}{2^{\alpha/2+j}}\Gamma\left(\frac{\alpha}{2}+j+1\right)}$$

$$= \frac{1}{2^{\alpha/2}} \frac{\Gamma(1+\alpha)}{\Gamma\left(\frac{\alpha}{2}-j+1\right)\Gamma\left(\frac{\alpha}{2}+j+1\right)}.$$

Thus, the coefficients c_j are given by

$$c_j = \frac{(-1)^j}{2^{\alpha/2}} \sum_{n=0}^{\infty} \binom{\alpha/2}{j+2n}\binom{j+2n}{n}\frac{1}{2^{j+2n}}$$

$$= \frac{(-1)^j}{2^\alpha} \frac{\Gamma(1+\alpha)}{\Gamma\left(\frac{\alpha}{2}-j+1\right)\Gamma\left(\frac{\alpha}{2}+j+1\right)} \tag{18}$$

for any $j \in \mathbb{N}$. Note, that setting $j=0$ in the above yields $c = c_0/2$, where c was given in (17). For $\alpha = 2k$, $k \in \mathbb{N}_0$ the binomial series expansion is only a finite sum and the coefficients c_j simplify to $c_j = \frac{(-1)^j}{4^k}\binom{2k}{k-j}$ for $j=0,\ldots,k$ and $c_j = 0$ for all $j > k$.

To summarize the Fourier series expansion of $\frac{1}{2}\left|\sin\left(\frac{x}{2}\right)\right|^{\alpha}$ is given by

$$\frac{1}{2}\left|\sin\left(\frac{x}{2}\right)\right|^{\alpha} = \frac{c_0}{2} + \sum_{j=1}^{\infty} c_j \cos(jx). \tag{19}$$

Absolute and uniform convergence of the above Fourier series for $\alpha \geqslant 0$ follow from [5, theorem 2.5] since $\frac{1}{2}|\sin(x/2)|^{\alpha}$ is π-periodic, continuous and piecewise smooth for $\alpha \geqslant 0$. For $-1 < \alpha < 0$ the function $\frac{1}{2}|\sin(x/2)|^{\alpha}$ is only π-periodic and piecewise smooth (with discontinuities at $x = 2k\pi$). The Fourier series converges at every point where the function is continuous [5, theorem 2.1].

(b) For $\alpha > -1$ consider the even extension of $f \in L^1_{w,\alpha}(\mathbb{R}_+)$ onto the whole $\mathbb{R}$. For ease of notation, we write $f \in L^1_{e,w,\alpha}(\mathbb{R})$. We make use of the Fourier expansion (19) of the integral kernel of T_{α}. Note that integration and summation can be interchanged by Lebesgue's dominated convergence theorem. Then,

$$T_{\alpha}f(y) = \int_0^{\infty} |\sin(xy)|^{\alpha} f(x)\mathrm{d}x = \int_{\mathbb{R}} \frac{1}{2}\left|\sin\left(\frac{2xy}{2}\right)\right|^{\alpha} f(x)\mathrm{d}x$$

$$= \frac{c_0}{2}\int_{\mathbb{R}} f(x)\mathrm{d}x + \sum_{j=1}^{\infty} c_j \int_{\mathbb{R}} \cos(2jxy)f(x)\mathrm{d}x$$

$$= \frac{c_0}{2}\mathcal{F}f(0) + \sum_{j=1}^{\infty} c_j \mathcal{F}f(2jy).$$

The case $\alpha = 2k$, $k \in \mathbb{N}_0$ follows immediately from the definition (14) of the coefficients c_j. $\square$

Corollary 2.

(a) *The series $\sum_{j=1}^{\infty} c_j$ converges absolutely for all $\alpha \geqslant 0$. In particular, for $\alpha > 0$ it holds that $\sum_{j=1}^{\infty} c_j = -\frac{c_0}{2}$, and in the case $\alpha \in (0, 2]$, the absolute limit is given by $\sum_{j=1}^{\infty} |c_j| = c_0/2$. For $-1 < \alpha < 0$, the series $\sum_{j=1}^{\infty} c_j$ diverges.*

(b) *For $\alpha \geqslant 0$, the convergence in the series representation of $T_{\alpha}f$, $f \in L^1(\mathbb{R}_+)$, in equation (15) is uniform. Consequently, $T_{\alpha}f$ is continuous and bounded for all $f \in L^1(\mathbb{R}_+)$, $\alpha \geqslant 0$. For $-1 < \alpha < 0$, convergence holds in the L^2-sense if $f \in L^1_{w,\alpha}(\mathbb{R}_+) \cap L^2(\mathbb{R}_+)$.*

Proof.

(a) The function $\frac{1}{2}\left|\sin\left(x/2\right)\right|^{\alpha}$ is 2π-periodic, continuous and piecewise smooth for $\alpha \geqslant 0$. Its Fourier series converges absolutely and uniformly on $\mathbb{R}$, in particular $\sum_{j=1}^{\infty} |c_j| < \infty$ [5, theorem 2.5]. Note that $T_{\alpha}f(0)$ is well-defined, and

$$T_{\alpha}f(0) = 0 = \frac{c_0}{2}\mathcal{F}f(0) + \sum_{j=1}^{\infty} c_j \mathcal{F}f(0) = \mathcal{F}f(0)\left(\frac{c_0}{2} + \sum_{j=1}^{\infty} c_j\right)$$

for $\alpha > 0$, hence $\sum_{j=1}^{\infty} c_j = -c_0/2$. For $\alpha \in (0, 2]$, it holds that $c_j \leqslant 0$ for all $j \geqslant 1$ by their definition, and consequently $\sum_{j=1}^{\infty} |c_j| = -\sum_{j=1}^{\infty} c_j = c_0/2$.

To show the divergence of $\sum_{j=1}^{\infty} c_j$ in the case $-1 < \alpha < 0$, note that

$$\Gamma\left(\frac{\alpha}{2} + j + 1\right) = \Gamma\left(\frac{\alpha}{2} + 2\right)\left(\frac{\alpha}{2} + 2\right)_{j-1},$$

and

$$\Gamma\left(\frac{\alpha}{2} - j + 1\right) = \frac{\Gamma\left(\frac{\alpha}{2}\right)}{\left(\frac{\alpha}{2} - j + 1\right)\left(\frac{\alpha}{2} - j + 2\right)\dots\left(\frac{\alpha}{2} - 1\right)} = \frac{\Gamma\left(\frac{\alpha}{2}\right)}{(-1)^{j-1}\left(1 - \frac{\alpha}{2}\right)_{j-1}},$$

where $(\cdot)_n$ is the Pochhammer symbol. Then,

$$\begin{aligned}
c_j &= \frac{(-1)^j}{2^\alpha}\frac{\Gamma(1+\alpha)}{\Gamma\left(\frac{\alpha}{2}+2\right)\left(\frac{\alpha}{2}+2\right)_{j-1}}\frac{(-1)^{j-1}\left(1-\frac{\alpha}{2}\right)_{j-1}}{\Gamma\left(\frac{\alpha}{2}\right)} \\
&= -\frac{\Gamma(1+\alpha)}{2^\alpha\Gamma\left(\frac{\alpha}{2}\right)\Gamma\left(\frac{\alpha}{2}+2\right)}\frac{\left(1-\frac{\alpha}{2}\right)_{j-1}(1)_{j-1}}{\left(\frac{\alpha}{2}+2\right)_{j-1}}\frac{1}{(j-1)!},
\end{aligned} \tag{20}$$

which yields

$$\sum_{j=1}^{\infty} c_j = -\frac{\Gamma(1+\alpha)}{2^\alpha\Gamma\left(\frac{\alpha}{2}\right)\Gamma\left(\frac{\alpha}{2}+2\right)}{}_2F_1\left[1-\frac{\alpha}{2}, 1; \frac{\alpha}{2}+2; 1\right].$$

The series diverges as $\frac{\alpha}{2} + 2 - \left(1 - \frac{\alpha}{2}\right) - 1 = \alpha \in (-1, 0)$, and since it holds that

$$\frac{\left(1-\frac{\alpha}{2}\right)_n(1)_n}{\left(\frac{\alpha}{2}+2\right)_n}\frac{1}{n!} = \frac{\Gamma\left(\frac{\alpha}{2}+2\right)}{\Gamma\left(1-\frac{\alpha}{2}\right)}n^{-\alpha-1}\left(1 + O\left(n^{-1}\right)\right),$$

with $n = j - 1$, where $-\alpha - 1 \in (-1, 0)$, cf [2, p 57].

(b) Define $T_\alpha^{(n)}f = \frac{c_0}{2}\mathcal{F}f(0) + \sum_{j=1}^{n} c_j\mathcal{F}f(2j\,\cdot)$. By (a) the Fourier coefficients satisfy $|c_j| \to 0$ as $j \to \infty$. Furthermore, $L_{w,\alpha}^1(\mathbb{R}_+) \subset L^1(\mathbb{R}_+)$ and $|\mathcal{F}f(y)| \leqslant 2\|f\|_1$ for all $y \in \mathbb{R}_+$, where $\|\cdot\|_1$ denotes the L^1-norm on $\mathbb{R}_+$.

Let $\alpha \geqslant 0$. Then,

$$\begin{aligned}
\lim_{n\to\infty}\left\|T_\alpha f - T_\alpha^{(n)}f\right\|_\infty &= \lim_{n\to\infty}\sup_{y\in\mathbb{R}_+}\left|T_\alpha f(y) - T_\alpha^{(n)}f(y)\right| \\
&= \lim_{n\to\infty}\sup_{y\in\mathbb{R}}\left|\sum_{j=n+1}^{\infty}c_j\mathcal{F}f(2jy)\right| \\
&\leqslant \lim_{n\to\infty}\sup_{y\in\mathbb{R}}\sum_{j=n+1}^{\infty}|c_j|\underbrace{|\mathcal{F}f(2jy)|}_{\leqslant 2\|f\|_1} \\
&\leqslant 2\|f\|_1\lim_{n\to\infty}\sum_{j=n+1}^{\infty}|c_j| = 0.
\end{aligned}$$

Since the Fourier transform $\mathcal{F}f$ is bounded and continuous for all integrable functions, continuity and boundedness of $T_\alpha f$ follow by the uniform convergence of the $T_\alpha^{(n)}f$.

Considering the case $-1 < \alpha < 0$, note that on the space $L^1_{w,\alpha}(\mathbb{R}_+) \cap L^2(\mathbb{R}_+)$ the Fourier transform $\mathcal{F}$ is an L^2-isometry [10, section 2.2.4], and by the Plancherel theorem the equality $\|\mathcal{F}f\|_2 = 2\pi\|f\|_2$ holds. Then,

$$
\lim_{n\to\infty} \left\| T_\alpha f - T_\alpha^{(n)} f \right\|_2^2 = \lim_{n\to\infty} \int_0^\infty \left| \sum_{j=n+1}^\infty c_j \mathcal{F}f(2jy) \right|^2 \mathrm{d}y
$$

$$
\leqslant \lim_{n\to\infty} \int_0^\infty \left(\sum_{j=n+1}^\infty |c_j|^2 |\mathcal{F}f(2jy)|^2 \right.
$$

$$
\left. + 2 \sum_{n+1<j<k}^\infty |c_j||c_k||\mathcal{F}f(2jy)||\mathcal{F}f(2jk)| \right) \mathrm{d}y
$$

$$
\leqslant \lim_{n\to\infty} \sum_{j=n+1}^\infty |c_j|^2 \underbrace{\int_0^\infty |\mathcal{F}f(2jy)|^2 \mathrm{d}y}_{\leqslant 2\pi\|f\|_2^2} + 2
$$

$$
\times \sum_{n+1<j<k}^\infty |c_j||c_k| \underbrace{\int_0^\infty |\mathcal{F}f(2jy)||\mathcal{F}f(2jk)|\mathrm{d}y}_{\leqslant 2\pi\|f\|_2^2}
$$

$$
= 0,
$$

where the last inequality is due to the Cauchy–Schwartz inequality. $\qquad\square$

For the boundedness of the integral operator T_α, in particular for the case $-1 < \alpha < 0$, we introduce the Sobolev space

$$
w^{1,1}(\mathbb{R}_+) = \left\{ f \in L^1(\mathbb{R}_+) : \exists\, f' \in L^1(\mathbb{R}_+) \right\}
$$

of integrable functions f with integrable first derivative f', and define the norm $\|\cdot\|_D$ on the space $L^1_{w,\alpha}(\mathbb{R}_+) \cap w^{1,1}(\mathbb{R}_+)$ by

$$
\|f\|_D = \int_{\mathbb{R}_+} |f(x)| \max\left\{ \frac{1}{x}, 1 \right\} \mathrm{d}x + \|f'\|_1.
$$

Moreover, consider the space $L^1([0,1], \mathrm{d}x) \cap C_b((1,\infty))$ with norm $\|\cdot\|_*$ defined by

$$
\|g\|_* = \int_0^1 |g(y)|\mathrm{d}y + \sup_{y>1}|g(y)|.
$$

Theorem 3.

(a) For $\alpha \geqslant 0$ the integral operator $T_\alpha : \left(L^1(\mathbb{R}_+), \|\cdot\|_1\right) \to \left(C_b(\mathbb{R}_+), \|\cdot\|_\infty\right)$ is a linear bounded (continuous) operator. In particular, for $\alpha \in (0,2]$, the operator norm is bounded by $\|T_\alpha\| \leqslant 2c_0$.

(b) *For $-1 < \alpha < 0$ the integral operator $T_\alpha : \left(L^1_{w,\alpha}(\mathbb{R}_+) \cap w^{1,1}(\mathbb{R}_+), \|\cdot\|_D\right) \to \left(L^1([0,1], dx) \cap C_b((1,\infty)), \|\cdot\|_*\right)$ is a linear bounded (continuous) operator. The operator norm is bounded by*

$$\|T_\alpha\| \leqslant C_\alpha \left(\frac{1}{\pi} + 1\right) + c_0 \left(1 - \frac{\alpha}{\alpha+2}{}_3F_2\left[1 - \frac{\alpha}{2}, 1, 1; \frac{\alpha}{2} + 2, 2; 1\right]\right),$$

with $C_\alpha = \sqrt{\pi} \dfrac{\Gamma\left(\frac{1+\alpha}{2}\right)}{\Gamma\left(1+\frac{\alpha}{2}\right)}$ and hypergeometric function ${}_3F_2$ as defined in equation (4).

Proof.   Linearity of T_α follows directly from the linearity of integrals. For the boundedness of T_α we consider the cases $\alpha \geqslant 0$ and $-1 < \alpha < 0$ separately.

(a) For $\alpha \geqslant 0$, use the inequality $|\mathcal{F}f(y)| \leqslant 2\|f\|_1$, $y \in \mathbb{R}_+$, to get

$$\|T_\alpha f\|_\infty = \left\|\frac{c_0}{2}\mathcal{F}f(0) + \sum_{j=1}^\infty c_j \mathcal{F}f(2j\cdot)\right\|_\infty \leqslant 2\|f\|_1 \left(\frac{c_0}{2} + \sum_{j=1}^\infty |c_j|\right) < \infty$$

and

$$\|T_\alpha\| = \sup_{f \in L^1(\mathbb{R}_+)\setminus\{0\}} \frac{\|T_\alpha f\|_\infty}{\|f\|_1} \leqslant 2\left(\frac{c_0}{2} + \sum_{j=1}^\infty |c_j|\right) < \infty,$$

where in the above 0 denotes the constant zero function. Following corollary 2(b) the upper bound of the operator norm of T_α for $\alpha \in (0,2]$ is then given by

$$\|T_\alpha\| \leqslant 2\left(\frac{c_0}{2} + \sum_{j=1}^\infty |c_j|\right) = 2c_0.$$

(b) Note that for $f \in C^n(\mathbb{R}_+)$ with integrable derivatives $f^{(k)} \in L^1(\mathbb{R}_+)$ for all $k \leqslant n$ the Fourier transform $\mathcal{F}f$ behaves as $O\left(\frac{1}{y^n}\right)$, $y \to \infty$. In particular, for $f \in w^{1,1}(\mathbb{R}_+)$ it follows that $|\mathcal{F}f(y)| = \frac{|\mathcal{F}f'(y)|}{|y|}$. Furthermore, $|c_j| = c_j$ since the coefficients c_j, $j \geqslant 0$, are positive for $-1 < \alpha < 0$ by their definition in equation (14), and from equation (20) in corollary 2(b) it holds that

$$\begin{aligned}
c_j &= -\frac{\Gamma(1+\alpha)}{2^\alpha \Gamma\left(\frac{\alpha}{2}\right)\Gamma\left(\frac{\alpha}{2}+2\right)} \frac{\left(1-\frac{\alpha}{2}\right)_{j-1}}{\left(\frac{\alpha}{2}+2\right)_{j-1}} \\
&= -\frac{\Gamma(1+\alpha)}{2^\alpha \Gamma\left(1+\frac{\alpha}{2}\right)^2} \frac{\alpha}{\alpha+2} \frac{\left(1-\frac{\alpha}{2}\right)_{j-1}}{\left(\frac{\alpha}{2}+2\right)_{j-1}} = -c_0 \frac{\alpha}{\alpha+2} \frac{\left(1-\frac{\alpha}{2}\right)_{j-1}}{\left(\frac{\alpha}{2}+2\right)_{j-1}}
\end{aligned} \tag{21}$$

for $j \geqslant 1$. With $j = \frac{(2)_{j-1}}{(1)_{j-1}}$ it follows that

$$\begin{aligned}
\sum_{j=1}^\infty \frac{|c_j|}{j} = \sum_{j=1}^\infty \frac{c_j}{j} &= -c_0 \frac{\alpha}{\alpha+2} \sum_{j=1}^\infty \frac{\left(1-\frac{\alpha}{2}\right)_{j-1}(1)_{j-1}(1)_{j-1}}{\left(\frac{\alpha}{2}+2\right)_{j-1}(2)_{j-1}} \times \frac{1}{(j-1)!} \\
&= -c_0 \frac{\alpha}{\alpha+2} \cdot {}_3F_2\left[1 - \frac{\alpha}{2}, 1, 1; \frac{\alpha}{2} + 2, 2; 1\right].
\end{aligned}$$

The above hypergeometric function series converges since $\frac{\alpha}{2} + 2 + 2 - \left(1 - \frac{\alpha}{2}\right) - 1 - 1 = 1 + \alpha > 0$ for all $-1 < \alpha < 0$.

Analogously to the proof of lemma 1 we can compute

$$
\int_0^1 |T_\alpha f(y)| \leqslant \int_0^\infty C_\alpha \left(\frac{1}{\pi} + \frac{1}{x}\right) |f(x)| \mathrm{d}x
$$

$$
= C_\alpha \left(\frac{1}{\pi} \underbrace{\|f\|_1}_{\leqslant \|f\|_D} + \underbrace{\int_0^\infty |f(x)| \frac{\mathrm{d}x}{x}}_{\substack{\leqslant \int_0^\infty |f(x)| \max\left\{\frac{1}{x}, 1\right\} \mathrm{d}x \\ \leqslant \|f\|_D}} \right)
$$

$$
\leqslant C_\alpha \left(\frac{1}{\pi} + 1\right) \|f\|_D,
$$

where $C_\alpha = \int_0^\pi |\sin(u)|^\alpha \mathrm{d}u = \sqrt{\pi} \frac{\Gamma\left(\frac{1+\alpha}{2}\right)}{\Gamma\left(1 + \frac{\alpha}{2}\right)}$. Moreover,

$$
\sup_{y>1} |T_\alpha f(y)| \leqslant \frac{c_0}{2} \underbrace{\mathcal{F}f(0)}_{=2\|f\|_1} + \sup_{y>1} \sum_{j=1}^\infty c_j |\mathcal{F}f(2jy)|
$$

$$
= c_0 \|f\|_1 + \sup_{y>1} \sum_{j=1}^\infty c_j \frac{1}{2jy} \underbrace{|\mathcal{F}f'(2jy)|}_{\leqslant 2\|f'\|_1}
$$

$$
\leqslant c_0 \|f\|_D + \sup_{y>1} \frac{1}{y} \|f'\|_1 \sum_{j=1}^\infty \frac{c_j}{j}
$$

$$
\leqslant c_0 \|f\|_D - \|f\|_D c_0 \frac{\alpha}{\alpha + 2} \cdot {}_3F_2 \left[1 - \frac{\alpha}{2}, 1, 1; \frac{\alpha}{2} + 2, 2; 1\right]
$$

$$
= \|f\|_D c_0 \left(1 - \frac{\alpha}{\alpha + 2} \cdot {}_3F_2 \left[1 - \frac{\alpha}{2}, 1, 1; \frac{\alpha}{2} + 2, 2; 1\right]\right).
$$

Ultimately, the operator norm is bounded by

$$
\|T_\alpha\| = \sup_{f \in (L^1_{w,\alpha}(\mathbb{R}_+) \cap w^{1,1}(\mathbb{R}_+)) \setminus \{0\}} \frac{\|T_\alpha f\|_*}{\|f\|_D}
$$

$$
\leqslant C_\alpha \left(\frac{1}{\pi} + 1\right) + c_0 \left(1 - \frac{\alpha}{\alpha + 2} \cdot {}_3F_2 \left[1 - \frac{\alpha}{2}, 1, 1; \frac{\alpha}{2} + 2, 2; 1\right]\right).
$$

$\square$

Similar to theorem 2, it is also possible to give a series representation of the α-*cosine transform on* $\mathbb{R}_+$, which we define by

$$
K_\alpha f(y) = \int_0^\infty |\cos(xy)|^\alpha f(x) \mathrm{d}x, \quad y \geqslant 0, \ f \in L^1_{w,\alpha}(\mathbb{R}_+). \tag{22}
$$

Corollary 3.   *Let $\alpha > -1$. Any function $f \in L^1_{w,\alpha}(\mathbb{R}_+)$ is mapped by K_α onto*

$$K_\alpha f(y) = \frac{\tilde{c}_0}{2} \mathcal{F}f(0) + \sum_{j=1}^{\infty} \tilde{c}_j \mathcal{F}f(2jy), \quad y \geqslant 0$$

with coefficients $\tilde{c}_j$, $j = 0, 1, \ldots,$ given by

$$\tilde{c}_j = (-1)^j c_j = \begin{cases} \dfrac{1}{2^\alpha} \dfrac{\Gamma(1+\alpha)}{\Gamma\left(\frac{\alpha}{2} - j + 1\right)\Gamma\left(\frac{\alpha}{2} + j + 1\right)}, & \alpha \neq 2k, \ j \in \mathbb{N}_0, \\[3mm] \dfrac{1}{4^k}\begin{pmatrix} 2k \\ k-j \end{pmatrix}, & \alpha = 2k, \ j = 0, \ldots, k, \ k \in \mathbb{N}_0, \\[3mm] 0, & \alpha = 2k, \ j > k, \ k \in \mathbb{N}_0. \end{cases}$$

Proof.   The result follows immediately from the equivalent formulation of the cosine double angle formula given by $\cos(2x) = 2\cos^2(x) - 1$, which yields

$$\frac{1}{2}\left|\cos\left(\frac{x}{2}\right)\right|^\alpha = \frac{1}{2}\left(\cos^2\left(\frac{x}{2}\right)\right)^{\alpha/2} = \frac{1}{2}\left(\frac{1+\cos(x)}{2}\right)^{\alpha/2}$$

$$= \frac{1}{2^{\alpha/2+1}} \sum_{k=0}^{\infty} \begin{pmatrix} \alpha/2 \\ k \end{pmatrix} \cos^k(x).$$

$\square$

Remark 2.   Counterparts of corollary 2 and theorem 3 for K_α follow immediately from $|\tilde{c}_j| = |c_j|$. The only exception is the convergence of the series $\sum_{j=1}^{\infty} \tilde{c}_j$ for $-1 < \alpha < 0$. This can be easily seen by the Leibniz criterion. More precisely, by equation (21) it holds that

$$\tilde{c}_j = (-1)^j c_j = (-1)^{j-1} c_0 \frac{\alpha}{\alpha + 2} \frac{\left(1 - \frac{\alpha}{2}\right)_{j-1}}{\left(\frac{\alpha}{2} + 2\right)_{j-1}},$$

hence

$$\sum_{j=1}^{\infty} \tilde{c}_j = c_0 \frac{\alpha}{\alpha + 2} \sum_{j=1}^{\infty} \frac{(1)_{j-1}\left(1 - \frac{\alpha}{2}\right)_{j-1}}{\left(\frac{\alpha}{2} + 2\right)_{j-1}} \frac{(-1)^{j-1}}{(j-1)!}$$

$$= c_0 \frac{\alpha}{\alpha + 2} \cdot {}_2F_1\left[1, 1 - \frac{\alpha}{2}; 2 + \frac{\alpha}{2}; -1\right].$$

The hypergeometric series above converges since $2 + \frac{\alpha}{2} - 1 - \left(1 - \frac{\alpha}{2}\right) + 1 = \alpha + 1 > 0$ for $\alpha \in (-1, 0)$.

4.2. Approximating the Fourier transform

Denote by $\hat{f} = \mathcal{F}f$ the Fourier transform of $f \in L^1_{e,w,\alpha}(\mathbb{R})$. Let $\hat{f}_R = \hat{f}\mathbb{1}\{|y| \leqslant R\}$, $R > 0$ be its restriction to $[-R, R]$. By the Fourier transform's symmetry it suffices to approximate $\hat{f}_R$ at equidistant points $\left\{n\frac{R}{N}\right\}$, $n = 1, \ldots, N$, $N \in \mathbb{N}$, from the series representation of $T_\alpha f$ in theorem 2. Define vectors $\boldsymbol{\xi}, \boldsymbol{\eta} \in \mathbb{R}^N$ with elements

$$\xi_n = \hat{f}_R\left(n\frac{R}{N}\right),$$

and

$$\eta_n = T_\alpha f\left(n\frac{R}{2N}\right) - \frac{c_0}{2}\mathcal{F}f(0)$$

for $n = 1, \ldots, N$, as well as the matrix $\boldsymbol{C} \in \mathbb{R}^{N \times N}$ with

$$\boldsymbol{C}_{i,j} = \begin{cases} c_k, & i < j \text{ with } j = ki \quad \text{for some } k \in \mathbb{N}. \\ 0, & \text{else,} \end{cases} \tag{23}$$

where the matrix elements c_k are the Fourier coefficients from theorem 2.

Proposition 1. *The vector $\boldsymbol{\xi}$ is uniquely determined by*

$$\boldsymbol{\xi} = \boldsymbol{C}^{-1} \cdot \boldsymbol{\eta}, \tag{24}$$

i.e. it is the unique solution of the system of linear equations $\boldsymbol{\eta} = \boldsymbol{C} \cdot \boldsymbol{\xi}$.

Proof. First note that $\hat{f}_R$ is continuous on the compact interval $[-R, R]$, as well as integrable and square-integrable on the real line. Furthermore, $\hat{f}_R$ converges in the L^2-norm to $\hat{f}$, hence $\mathcal{F}^{-1}\hat{f}_R \to \mathcal{F}^{-1}\hat{f} = f$ in the L^2-norm as $R \to \infty$. By the Riemann–Lebesgue lemma, the Fourier transform $\hat{f}$ is bounded, uniformly continuous, and vanishes at infinity [10], hence we approximate $\hat{f}$ by $\hat{f}_R$ in equation (15) with R chosen large enough. Then,

$$\eta_n = T_\alpha f\left(n\frac{R}{2N}\right) - \frac{c_0}{2}\mathcal{F}f(0) = \sum_{j=1}^{\infty} c_j \hat{f}\left(2jn\frac{R}{2N}\right)$$

$$\approx \sum_{j=1}^{\lfloor N/n \rfloor} c_j \hat{f}_R\left(jn\frac{R}{N}\right) = \sum_{j=1}^{\lfloor N/n \rfloor} c_j \xi_{jn}$$

for $n = 1, \ldots, N$ forms a system of linear equations, which in matrix form is given by

$$\boldsymbol{\eta} = \boldsymbol{C} \cdot \boldsymbol{\xi},$$

where $\boldsymbol{C} = \left(\boldsymbol{C}_{i,j}\right)_{i,j=1,\ldots,N}$ with $\boldsymbol{C}_{i,j}$ as in equation (23), i.e.

$$\boldsymbol{C} = \begin{pmatrix} c_1 & c_2 & c_3 & c_4 & c_5 & c_6 & c_7 & c_8 & c_9 & \cdots & c_{N-2} & c_{N-1} & c_N \\ 0 & c_1 & 0 & c_2 & 0 & c_3 & 0 & c_4 & 0 & \cdots & c_{N/2-1} & 0 & c_{N/2} \\ 0 & 0 & c_1 & 0 & 0 & c_2 & 0 & 0 & c_3 & \cdots & \cdots & \cdots & \cdots \\ 0 & 0 & 0 & c_1 & 0 & 0 & 0 & c_2 & 0 & \cdots & \cdots & \cdots & \cdots \\ \vdots & & & & \ddots & & & & & & & & \\ \vdots & & & & & & & & & & & & \\ \vdots & & & & & & & & & 0 & \cdots & c_1 & 0 \\ 0 & \cdots & & & & & & & & & \cdots & 0 & c_1 \end{pmatrix}.$$

In the illustration of the matrix $\boldsymbol{C}$ above it is assumed, without loss of generality, that N is an even integer. By the construction of the system of linear equations, $\boldsymbol{C}$ is an upper triangular matrix with non-zero entries c_1 on its main diagonal. In particular, this means that its inverse $\boldsymbol{C}^{-1}$ exists, and $\boldsymbol{\xi}$ is uniquely determined by

$$\boldsymbol{\xi} = \boldsymbol{C}^{-1} \cdot \boldsymbol{\eta}. \qquad \square$$

4.3. Band-limited interpolation

We aim to reconstruct the Fourier transform $\hat{f}$ with a suitable interpolation. In the previous subsection we introduced the vector $\boldsymbol{\xi}$ with coordinates $\xi_n = \hat{f}(nR/N)$, $n = 1, \ldots, N$. Set $\hat{f}(-nR/N) = \hat{f}(nR/N)$ and $\hat{f}(0) = \mathcal{F}f(0)$, which we assume to be known for now. Note that this is in general not true. A simple workaround solving this is discussed in section 6. Moreover, in the application examples of section 5, the value $\mathcal{F}f(0)$ is further specified.

Define the band-limited interpolation of the Fourier transform $\hat{f}$ by

$$\widehat{f_R^{(N)}} = \sum_{n=-N}^{N} \hat{f}\left(n\frac{R}{N}\right) \operatorname{sinc}\left(\frac{N}{R}y - n\right), \tag{25}$$

where $\operatorname{sinc}(x) = \sin(\pi x)/(\pi x)$ for $x \neq 0$ and $\operatorname{sinc}(0) = 1$. Furthermore, define the estimate

$$f_R^{(N)}(x) = \frac{R}{2\pi N} \operatorname{rect}\left(\frac{xR}{2\pi N}\right) \sum_{n=-N}^{N} \hat{f}\left(n\frac{R}{N}\right) \mathrm{e}^{-\mathrm{i}xnR/N}, \tag{26}$$

where

$$\operatorname{rect}(t) = \begin{cases} 1, & |t| < 1/2, \\ 0, & |t| > 1/2, \\ 1/2 & t = 1/2. \end{cases}$$

Theorem 4. *Let $f \in L^1_{e,w,\alpha}(\mathbb{R}) \cap L^2_e(\mathbb{R})$ and $B = N/(2R)$. Additionally, assume that $f \in C_e(\mathbb{R})$ with integrable first derivative $f' \in L^1_e(\mathbb{R})$.*

(a) The band-limited interpolation $\widehat{f_R^{(N)}}$ converges to $\hat{f}$ in the L^2-norm, i.e. it holds that

$$\lim_{B\to\infty} \lim_{N\to\infty} \left\| \hat{f} - \widehat{f_R^{(N)}} \right\|_2 = 0.$$

(b) The estimate $f_R^{(N)}(x)$ converges to f in the L^2-norm. It holds that

$$\lim_{B\to\infty} \lim_{N\to\infty} \left\| f - f_R^{(N)} \right\|_2 = 0.$$

Proof.

(a) Define the cardinal series of $\hat{f}$ by

$$S_B \hat{f}(y) = \sum_{n=-\infty}^{\infty} \hat{f}\left(\frac{n}{2B}\right) \operatorname{sinc}(2By - n).$$

The *Whittaker–Shannon–Kotel'nikov sampling theorem* [3, 14, 22, 25], widely known in the field of sampling theory, states that any bandlimited function u, i.e. $u \in L^p(\mathbb{R})$, $1 \leqslant p < \infty$, with compactly supported Fourier transform $\hat{u}$ on $[-B, B]$, can be completely reconstructed in from its cardinal series $S_B u$ in L^p [22, theorem 6]. The optimal sampling rate $2B$ is called *Nyquist-rate*. In our case $u = \hat{f}$.

Denote by

$$S_B^{(N)} \hat{f}(y) = \sum_{n=-N}^{N} \hat{f}\left(\frac{n}{2B}\right) \operatorname{sinc}(2By - n), \tag{27}$$

the truncated cardinal series of $\widehat{f}$. Suppose that $\hat{f}$ is band-limited, i.e. the function $f \in L^1_{e,w,\alpha}(\mathbb{R}) \cap L^2_e(\mathbb{R})$ has compact support $[-B, B]$ for some $B > 0$. Then, $\hat{f} \in L^2_e(\mathbb{R})$ is completely determined by its cardinal series $S_B\hat{f}$, and

$$S_B^{(N)}\hat{f} \to S_B\hat{f} = \hat{f}, \tag{28}$$

in the L^2-sense as $N \to \infty$.

The assumption that f has compact support is certainly too strong, and the Shannon sampling theorem applied to non-bandlimited functions will result in interpolation errors known as *aliasing*. To ensure L^2-convergence of the bandlimited interpolation when $\hat{f}$ is not band-limited, we refer to the results in [18]. For $p > 1$, define

$$\mathcal{F}^p(\delta) = \left\{ u : \mathbb{R} \to \mathbb{C} \text{ measurable}, u(x) = O\left(\frac{1}{\left(1 + |x|\right)^{1/p+\delta}} \right) \right\},$$

and $\mathcal{F}^p = \cup_{\delta>0}\mathcal{F}^p(\delta)$. Denote by $\mathcal{R}$ the set of all measurable functions $g : \mathbb{R} \to \mathbb{C}$ that are Riemann-integrable on every finite interval. Then,

$$\|u - S_B u\|_p \to 0$$

as $B \to \infty$ for all $g \in \mathcal{F}^p \cap \mathcal{R}$. We need $\left\| \hat{f} - S_B\hat{f} \right\|_{L^2} \to 0$ as $B \to \infty$, i.e. $\hat{f} \in \mathcal{F}^2(\delta)$ needs to hold for some $\delta > 0$.

Recall, that for any function $f \in C^n(\mathbb{R})$ with integrable derivatives $f^{(k)} \in L^1(\mathbb{R})$ for all $k \leqslant n$, its Fourier transform $\hat{f}$ decays as $O\left(\frac{1}{(1+|y|)^n} \right)$, $|y| \to \infty$. Setting $n = 1$ yields the desired result if additionally to $f \in L^1_{e,w,\alpha}(\mathbb{R}) \cap L^2_e(\mathbb{R})$ it is assumed that $f \in C^1_e(\mathbb{R})$ with integrable first derivative $f' \in L^1_e(\mathbb{R})$. Then, $\hat{f}(y) = O\left(1/(1 + |y|)^{1/2+\delta}\right)$ with $\delta = 1/2$. Furthermore, $\hat{f}$ is uniformly continuous on $\mathbb{R}$ and bounded, in particular it is integrable over all finite intervals. Hence,

$$\left\| \hat{f} - S_B\hat{f} \right\|_2 \to 0$$

as $B \to \infty$, i.e. the cardinal series $S_B\hat{f}$ converges to $\hat{f}$ in the L^2-norm. The above and the L^2-convergence in (28) imply that

$$\lim_{B\to\infty} \lim_{N\to\infty} \left\| \hat{f} - S_B^{(N)}\hat{f} \right\|_2 \leqslant \lim_{B\to\infty} \lim_{N\to\infty} \left(\left\| \hat{f} - S_B\hat{f} \right\|_2 + \left\| S_B\hat{f} - S_B^{(N)}\hat{f} \right\|_2 \right) = 0.$$

Setting $2B = N/R$ in the truncated cardinal series (27) yields the interpolant

$$\widehat{f_R^{(N)}} = \sum_{n=-N}^{N} \hat{f}\left(n\frac{R}{N} \right) \text{sinc}\left(\frac{N}{R}y - n \right).$$

(b) Note that

$$\left\{ \mathcal{F}^{-1} \text{sinc}\left(2B \cdot -n\right) \right\}(x) = \frac{1}{4\pi B} \text{rect}\left(\frac{x}{4\pi B} \right) e^{-ixn/(2B)},$$

and applying the inverse Fourier transform $\mathcal{F}^{-1}$ to the band-limited interpolation $\widehat{f_R^{(N)}}$ yields

$$f_R^{(N)}(x) = \frac{R}{2\pi N} \operatorname{rect}\left(\frac{xR}{2\pi N}\right) \sum_{n=-N}^{N} \hat{f}\left(n\frac{R}{N}\right) \mathrm{e}^{-\mathrm{i}xnR/N}.$$

As the L^2-convergence of the interpolant to $\hat{f}$ is preserved under the inverse Fourier transform, we ultimately get

$$\lim_{B\to\infty} \lim_{N\to\infty} \left\| f - f_R^{(N)} \right\|_2 = 0.$$

Remark 3.

(a) Under the assumptions of theorem 4 the cardinal series $S_B\hat{f}$ converges uniformly to $\hat{f}$ as $B \to \infty$ with error estimate

$$\left\| \hat{f} - S_B\hat{f} \right\|_\infty \leqslant \frac{1}{\pi} \int_{|x|>B} |f(x)|\mathrm{d}x.$$

This is a direct consequence of [4, theorem 1].

(b) Alternatively, it is also possible to use piecewise linear interpolation. Denote by $\hat{f}_{N,R}$ the piecewise linear interpolation polynomial constructed from the interpolation points $\boldsymbol{\xi} = \left(\hat{f}(kR/N)\right)_{k=-N}^{N}$ of proposition 1. It is well known that the Fourier transform $\hat{f}$ is n-times continuously differentiable if the function f is piecewise continuous and $x^k f(x)$ is integrable for all $k \leqslant n$ [13]. Restricted to compact intervals, boundedness follows.

Hence, if $f \in L^1_{e,w,\alpha}$ is additionally assumed to satisfy $xf(x), x^2 f(x) \in L^1(\mathbb{R})$, then $\hat{f}$ is twice continuously differentiable. It follows that linear interpolation $\hat{f}_{N,R}$ converges to $\hat{f}_R$ uniformly as $N \to \infty$, and the error estimate

$$\left\| \hat{f}_R - \hat{f}_{N,R} \right\|_\infty \leqslant C\left(\frac{R}{N}\right)^2 \left\| (\hat{f}_R)'' \right\|_\infty$$

holds, where C is some positive constant [17, chapter 8.3] and $(\hat{f}_R)''$ denotes the second derivative of $\hat{f}_R$. This implies convergence in the L^2-norm over $[0, R]$ which is preserved by the Fourier transform, thus

$$\mathcal{F}^{-1}\hat{f}_{N,R} \to \mathcal{F}^{-1}\hat{f}_R$$

in the L^2-norm as $N \to \infty$. Furthermore, $\mathcal{F}^{-1}\hat{f}_{N,R} \to \mathcal{F}^{-1}\hat{f}_R$ in the L^2-norm as $N \to \infty$.

4.4. Smoothing

In applications, there is a possibility that the function $T_\alpha f$ is contaminated by noise, which directly affects the solution of the linear equation $\boldsymbol{\eta} = \boldsymbol{C} \cdot \boldsymbol{\xi}$ from proposition 1. To cope with noisy data of $T_\alpha f$, we fix a non-negative, even *mollifier function* $e_\gamma(x)$, $\gamma > 0$, that integrates to 1, and converges to the Dirac-delta function as γ tends to 0. Additionally, determine the respective *reconstruction kernel* ψ_γ by the relationship $\psi_\gamma = \mathcal{F}e_\gamma$. Suitable mollifiers and their

respective reconstruction kernels are given in example 2 of section 6.2.1. A smoothed estimate of f can then be computed by the following proposition.

Proposition 2.   *Under the assumptions of theorem 4, a smoothed estimate of f is given by*

$$f_{R,\gamma}^{(N)} = \mathcal{F}^{-1}\left(\widehat{f_R^{(N)}} \cdot \psi_\gamma\right) \to f \tag{29}$$

as $\gamma \to 0, N \to \infty, R \to \infty$, where $\widehat{f_R^{(N)}} = S_B$ is the interpolation given in equation (25). The convergence to the function f is understood in the L^2-sense. Uniform convergence is guaranteed if $f \in C_b(\mathbb{R})$.

Proof.   For a given mollifier e_γ we consider the convolution

$$f_\gamma(x) = \left(f * e_\gamma\right)(x) = \mathcal{F}^{-1}\left(\mathcal{F}f \cdot \mathcal{F}e_\gamma\right)(x) = \mathcal{F}^{-1}\left(\hat{f} \cdot \psi_\gamma\right)(x), \tag{30}$$

which converges to the function f in the L^2-norm as $y \to \infty$ since $f \in L_e^2(\mathbb{R})$. Uniform convergence is guaranteed if $f \in C_b(\mathbb{R})$ [10, theorem 1.2.19]. Applying (30) to $\widehat{f_R^{(N)}}$, we then compute the smoothed estimate

$$f_{R,\gamma}^{(N)} = \mathcal{F}^{-1}\left(\widehat{f_R^{(N)}} \cdot \psi_\gamma\right),$$

where L^2-convergence is preserved by the inverse Fourier transform. $\square$

5. Applications

In the following section, we briefly present two applications for the inversion of α-sine and cosine transforms. First, harmonizable symmetric α-stable processes as well as their connection to α-sine transforms are outlined. The theory of complex stable measures and stochastic integrals can be quite technical, and a detailed discussion would go beyond the scope of this work. We refer to [21] for a complete introduction to these processes. The second application deals with the inversion of the two-dimensional spherical α-cosine transform.

5.1. Stationary real harmonizable symmetric α-stable processes

Consider a probability space $(\Omega, \mathcal{F}, P)$. Define the spaces $L^0(\Omega)$ and $L_c^0(\Omega)$ of real-valued and complex valued random variables on this probability space, respectively. Then, every element $X \in L_c^0(\Omega)$ is of the form $X = X_1 + iX_2$ with $X_1, X_2 \in L^0(\Omega)$. A real-valued *symmetric α-stable random variable* $X \sim S\alpha S(\sigma)$ on this probability space is defined by the characteristic function

$$\mathbb{E}\left[e^{isX}\right] = \exp\left\{-\sigma^\alpha |s|^\alpha\right\},$$

where $\sigma > 0$ is called the *scale parameter* of X and $\alpha \in (0, 2]$ its *index of stability*. In the multivariate case, a real-valued symmetric α-stable random vector $X = (X_1, \ldots, X_n)$ is defined by its joint characteristic function

$$\mathbb{E}\left[\exp\left\{i(s, X)\right\}\right] = \exp\left\{-\int_{S^{n-1}} |(\theta, s)|^\alpha \Gamma(d\theta)\right\},$$

where $(\boldsymbol{x}, \boldsymbol{y})$ denotes the scalar product of two vectors $\boldsymbol{x}, \boldsymbol{y} \in \mathbb{R}^n$, and S^{n-1} is the unit sphere in $\mathbb{R}^n$. The measure Γ is called the *spectral measure* of X. It is unique, finite and symmetric in the case $0 < \alpha < 2$ [21, theorem 2.4.3].

Let us define the notion of complex random measure. Let $(E, \mathcal{E})$ be a measurable space, and let $(S^1, \mathcal{B}(S^1))$ be the measurable space on the unit circle S^1 equipped with the Borel σ-algebra $\mathcal{B}(S^1)$. Let k be a measure on the product space $(E \times S^1, \mathcal{E} \times \mathcal{B}(S^1))$, and let

$$\mathcal{E}_0 = \left\{ A \in \mathcal{E} : k(A \times S^1) < \infty \right\}.$$

A *complex-valued SαS random measure* on $(E, \mathcal{E})$ is an independently scattered, σ-additive, complex-valued set function

$$M : \mathcal{E}_0 \to L_c^0(\Omega)$$

such that the real and imaginary part of $M(A)$, i.e. the vector $(M^{(1)}(A), M^{(2)}(A)) = (\mathrm{Re}(M(A)), \mathrm{Im}(M(A)))$, is jointly S$\alpha$S with spectral measure $k(A \times \cdot)$ for every $A \in \mathcal{E}_0$ [21, definition 6.1.2]. We refer to k as the *circular control measure* of M, and denote by $m(A) = k(A \times S^1)$ the *control measure* of M. Furthermore, M is isotropic if and only if its circular control measure is of the form

$$k = m\gamma,$$

where γ is the uniform probability measure on S^1.

A stochastic integral with respect to a complex SαS random measures M is defined by

$$I(u) = \int_E u(x) M(\mathrm{d}x),$$

where $f : E \to \mathbb{C}$ is a measurable, complex-valued function from the space $L^\alpha(E, m)$. The integral $I(u)$ is well-defined by [21, proposition 6.2.2].

Let $(E, \mathcal{E}) = (\mathbb{R}, \mathcal{B})$ and $u(t, x) = \mathrm{e}^{\mathrm{i}tx}$. Then, the stochastic process $\{X(t) : t \in \mathbb{R}\}$ defined by

$$X(t) = \mathrm{Re}\left(I\left(u(t, \cdot)\right)\right) = \mathrm{Re}\left(\int_{\mathbb{R}} \mathrm{e}^{\mathrm{i}tx} M(\mathrm{d}x)\right),$$

where M is a complex SαS random measure on $(\mathbb{R}, \mathcal{B})$ with finite circular control measure k (equivalently, with finite control measure m), is called a *real harmonizable SαS process*.

By [21, theorem 6.5.1], this process is stationary if and only if M is isotropic, i.e. its spectral measure is of the form $k = m\gamma$. For all $n \in \mathbb{N}$ and $t_1, \ldots, t_n \in \mathbb{R}$, the characteristic function of the finite-dimensional distributions of the process X is given by

$$\mathbb{E}\left[\exp\left\{i\sum_{i=1}^n s_i X_{t_i}\right\}\right] = \exp\left\{-\lambda_\alpha \int_{\mathbb{R}} \left|\sum_{j,k=1}^n s_j s_k \cos\left((t_k - t_j)x\right)\right|^{\alpha/2} m(\mathrm{d}x)\right\} \tag{31}$$

with constant $\lambda_\alpha = \frac{1}{2\pi}\int_0^{2\pi} |\cos(x)|^\alpha \mathrm{d}x$, see [21, proposition 6.6.3].

The *codifference function* $\tau(t)$ of a SαS stochastic process is defined as the codifference of the random variables X_0 and X_t, i.e.

$$\tau(t) = \|X_0\|_\alpha^\alpha + \|X_t\|_\alpha^\alpha - \|X_t - X_0\|_\alpha^\alpha, \tag{32}$$

where $\| \cdot \|_\alpha$ is the scale parameter of X_0, X_t and $X_t - X_0$, respectively.

5.2. Problem setting and inversion

Let $X = \{X_t : t \in \mathbb{R}\}$ be a stationary real harmonizable $S\alpha S$ process with finite circular control measure k, and suppose its control measure m has an even, non-negative density function $f \in L_e^1(\mathbb{R}) \cap L_e^2(\mathbb{R})$ with respect to the Lebesgue measure on $\mathbb{R}$. We refer to the function f as the *spectral density*. It follows that $m(\mathrm{d}x) = f(x)\mathrm{d}x$ in equation (31), and the random variables X_0, X_t and $X_t - X_0$ in (32) are $S\alpha S$ random variables with the following scale parameters.

First, it holds that $X_t \sim S\alpha S(\sigma)$ with

$$\sigma = \left(\lambda_\alpha \int_{\mathbb{R}} f(x)\mathrm{d}x \right)^{1/\alpha} = (\lambda_\alpha m(\mathbb{R}))^{1/\alpha}.$$

In particular, this yields $m(\mathbb{R}) = \sigma^\alpha / \lambda_\alpha$. By stationarity of X, the random variable X_0 has the same scale parameter σ.

Similarly, for $X_t - X_0$ equation (31) yields

$$\mathbb{E}\left[is\, (X_t - X_0) \right] = \exp\left\{ -\lambda_\alpha \int_{\mathbb{R}} |s^2\, (2 - \cos(tx) - \cos(-tx))|^{\alpha/2} f(x)\mathrm{d}x \right\}$$

$$= \exp\left\{ -|s|^\alpha \lambda_\alpha \left(\int_{\mathbb{R}} |2 - 2\,\cos(tx)|^{\alpha/2} f(x)\mathrm{d}x \right) \right\}$$

$$= \exp\left\{ -|s|^\alpha 2^\alpha \lambda_\alpha \left(\int_{\mathbb{R}} \left| \sin\left(\frac{tx}{2} \right) \right|^\alpha f(x)\mathrm{d}x \right) \right\}.$$

It follows that $X_t - X_0 \sim S\alpha S(\tilde{\sigma})$ with

$$\tilde{\sigma} = 2 \left(\lambda_\alpha \int_{\mathbb{R}} \left| \sin\left(\frac{tx}{2} \right) \right|^\alpha f(x)\mathrm{d}x \right)^{1/\alpha}.$$

Ultimately, the codifference function in equation (32) expands to

$$\tau(t) = 2\sigma^\alpha - \tilde{\sigma}^\alpha = 2\sigma^\alpha - 2^\alpha \lambda_\alpha \int_{\mathbb{R}} \left| \sin\left(\frac{tx}{2} \right) \right|^\alpha f(x)\mathrm{d}x.$$

Suppose that the spectral density f is an even, integrable function. Then rearranging the above yields

$$T_\alpha f\, (t) = \int_0^\infty |\sin\, (tx)|^\alpha f(x)\mathrm{d}x = \frac{2\sigma^\alpha - \tau(2t)}{2^{\alpha+1}\lambda_\alpha} =: g(t). \tag{33}$$

Assume that the scale parameter σ, the index of stability $\alpha \in (0, 2)$ and the codifference function τ are known. Then, $\mathcal{F}f(0) = m(\mathbb{R}) = \sigma^\alpha / \lambda_\alpha$. Furthermore, set $\boldsymbol{\eta} = (\eta_1, \ldots, \eta_N)$ with $\eta_n = g\left(n\frac{R}{2N} \right) - \frac{c_0 \sigma^\alpha}{2\lambda_\alpha}$, $n = 1, \ldots, N$, and solve the system of linear equations $\boldsymbol{\eta} = \boldsymbol{C}\boldsymbol{\xi}$, where

$\boldsymbol{\xi} = (\xi_1, \ldots, \xi_N)$ with $\xi_n = \hat{f}\left(n\frac{R}{N}\right)$, $n = 1, \ldots, N$. Apply theorem 4 to compute the estimate of the spectral density f.

Remark 4. In statistical inference, the scale parameter σ, the index of stability $\alpha \in (0, 2)$ and the codifference function τ need to be estimated from a realization of the process X.

5.3. Two-dimensional spherical α-cosine transform

As mentioned in the introduction before, spherical α-cosine transforms are of particular interest in stochastic and convex geometry. For example, when analyzing fiber processes, the so-called rose of intersections is closely related to the α-cosine transform of the underlying directional distribution of the fibers. Also, in convex geometry, the support function of a zonoid is the spherical α-cosine transform of some generating measure ρ.

Let f be an even, integrable function on S^n (i.e. the unit sphere in $\mathbb{R}^{n+1}$) with respect to the area surface measure on S^n. We write $f \in L^1_e(S^n)$. Define the $(n + 1)$-*dimensional spherical α-cosine transform* of f by $K_{\alpha, S^n} : L^1_e(S^n) \to C_e(S^n)$ with

$$K_{\alpha, S^n} f(\boldsymbol{\eta}) = \int\limits_{S^n} |(\boldsymbol{\theta}, \boldsymbol{\eta})|^\alpha f(\boldsymbol{\theta}) \mathrm{d}\boldsymbol{\theta}, \quad \boldsymbol{\eta} \in S^n, \tag{34}$$

where $(\cdot, \cdot)$ denotes the inner product of the vectors $\boldsymbol{\theta}, \boldsymbol{\eta} \in S^n$. The spherical α-cosine transform is well-defined for $\alpha > -1$, see [19].

Every point $\boldsymbol{\theta} = (\cos(x), \sin(x))$ on the unit circle S^1 corresponds one-to-one to an angle $x \in (-\pi, \pi]$, and any function $f \in L^1(S^1)$ can be parameterized as a 2π-periodic function on $\mathbb{R}$, which is integrable over $[-\pi, \pi]$. We simply denote this by $f \in L^1([-\pi, \pi])$. It is π-periodic if f is even on S^1. Furthermore, the inner product of $\boldsymbol{\theta}, \boldsymbol{\eta} \in S^1$ is equivalent to the cosine of the angle between those two vectors. Define the convolution of 2π-periodic functions $u, v \in L^2([-\pi, \pi])$ by

$$(u * v)(t) = \int\limits_{-\pi}^{\pi} u(t - x)v(x)\mathrm{d}x = \int\limits_{-\pi}^{\pi} u(x)v(t - x)\mathrm{d}x, \quad t \in [-\pi, \pi].$$

Any 2π-periodic function $u \in L^2([-\pi, \pi])$ has the Fourier series expansion (in exponential form)

$$u(x) = \sum_{n=-\infty}^{\infty} \hat{u}(n)\mathrm{e}^{\mathrm{i}nx}$$

with Fourier coefficients

$$\hat{u}(n) = \frac{1}{2\pi} \int\limits_{-\pi}^{\pi} \mathrm{e}^{-\mathrm{i}nx} u(x)\mathrm{d}x.$$

The convolution theorem of Fourier coefficients states that $\widehat{(u * v)}(n) = 2\pi\hat{u}(n)\hat{v}(n)$ for all $u, v \in L^2([-\pi, \pi])$. Furthermore, the Fourier coefficient of the translation of u by a constant $h \in \mathbb{R}$ is given by $\widehat{u(\cdot - h)}(n) = \hat{u}(n)\mathrm{e}^{-\mathrm{i}nh}$.

Then, the two-dimensional equivalent of (34) on S^1 is defined by

$$K_{\alpha,S^1} f(y) = \int_{-\pi}^{\pi} |\cos(y-x)|^\alpha f(x) \mathrm{d}x = \left(|\cos(\cdot)|^\alpha * f \right)(y), \quad y \in [-\pi, \pi]. \tag{35}$$

Corollary 4. *Let* $\alpha > -1$, $\alpha \neq 0, 2, 4, \ldots$. *Let* $f \in L^2([-\pi, \pi])$ *be a* π-*periodic probability density function. Then, f can be completely reconstructed from its Fourier coefficients by*

$$f(x) = \frac{1}{2\pi} \left(1 + \sum_{n \in \mathbb{Z} \setminus \{0\}} \frac{\widehat{(K_{\alpha,S}f)}(2n)}{\tilde{c}_{|n|}} \mathrm{e}^{\mathrm{i}2nx} \right) \tag{36}$$

for all $x \in [-\pi, \pi]$, *where the coefficients* $\tilde{c}_k$, $k = 0, 1, \ldots$, *are given in corollary* 3.

Proof. Since $\{\tilde{c}_n\}$ are the coefficients of the Fourier series (in sine–cosine form) of the function $\frac{1}{2} \left| \cos \left(\frac{x}{2} \right) \right|^\alpha$, one can easily verify that $\widehat{|\cos(\cdot)|^\alpha}(n) = \tilde{c}_{|n/2|}$ for even $n \in \mathbb{Z}$ and 0 otherwise. Thus, by the convolution theorem and equation (35) we get the Fourier coefficients $\widehat{K_{\alpha,S^1}}(n) = 2\pi c_{|n/2|} \hat{f}(n)$ for even $n \in \mathbb{Z}$ and 0 otherwise, as well as the series expansion

$$K_{\alpha,S^1} f(y) = 2\pi \sum_{n=-\infty}^{\infty} \tilde{c}_{|n|} \hat{f}(2n) \mathrm{e}^{\mathrm{i}2ny}.$$

Note that $\hat{f}(0) = 1/(2\pi)$, and for any even $n \in \mathbb{N}$ we can compute $\hat{f}(n) = \widehat{K_{\alpha,S^1}f}(n)/(2\pi c_{n/2})$. Moreover, since f is π-periodic, there exists a shift $h \in [0, \pi]$ such that $f^*(x) = f(x + h)$ is an even, π-periodic function. It holds that

$$\hat{f}^*(n) = \frac{1}{2\pi} \int_{-\pi}^{\pi} \mathrm{e}^{-\mathrm{i}nx} f^*(x) \mathrm{d}x = \frac{1}{\pi} \int_0^{\pi} \cos(nx) f^*(x) \mathrm{d}x = 0$$

since $\cos(n\cdot)$ is odd about $\pi/2$ on $[0, \pi]$ for all odd $n \in \mathbb{N}$. By the shift property we get $\hat{f}(n) = \hat{f}^*(n)\mathrm{e}^{-\mathrm{i}nh} = 0$ for n odd.

To summarize the Fourier coefficients of f are given by

$$\hat{f}(n) = \begin{cases} 1/(2\pi) & n = 0 \\ \widehat{K_{\alpha,S^1}f}(n)/(2\pi\tilde{c}_{n/2}), & n = 2k, \ k \in \mathbb{N}, \\ 0 & n = 2k+1, \ k \in \mathbb{N}. \end{cases} \tag{37}$$

Lastly, note that $\hat{f}(-n) = \overline{\hat{f}(n)}$, where $\bar{z}$ denotes the complex conjugate for $z \in \mathbb{C}$. Applying this to the Fourier series representation $f(x) = \sum_{n=-\infty}^{\infty} \hat{f}(n)\mathrm{e}^{\mathrm{i}nx}$ yields the desired result. $\qquad\square$

Remark 5. In the case $\alpha = 0, 2, 4, \ldots$, the coefficients $\tilde{c}_j = 0$ for all $j \geqslant \alpha/2$ (see corollary 3). Thus, only a finite number of Fourier coefficients of f can be computed from the Fourier coefficients $\widehat{K_{\alpha,S}f}(n)$, making it impossible to fully reconstruct f.
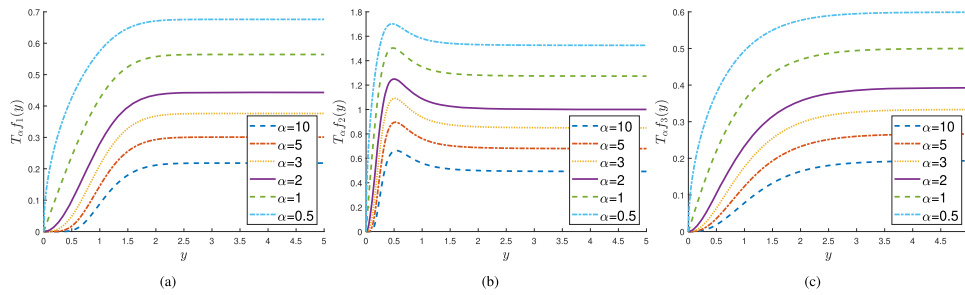
Figure 1. α-sine transform on $\mathbb{R}$. Plots of the function Tf for all three examples f_1, f_2 and f_3 with $\alpha \in \{0.5, 1, 2, 3, 5, 10\}$.

6. Numerical results

We first consider the α-sine transform on $\mathbb{R}_+$. The inversion results of the direct approach are presented in section 6.1 for the case $\alpha > 1$. Additionally, various numerical difficulties that emerge when dealing with the direct approach are analyzed. The Fourier approximation approach is considered in section 6.2. It proves to be more accurate as well as more efficient compared to the direct approach. Most importantly, it is applicable for all $\alpha > -1$. Inversion results are first shown for $\alpha \geqslant 0$, the case $-1 < \alpha < 0$ is considered separately. Moreover, in the context of an application to harmonizable $S\alpha S$ processes, Gaussian noise is added to the transform $T_\alpha f$ to test the smoothing procedure of section 4.4. Lastly, section 6.3 deals with the two dimensional α-cosine transform. We consider a number of π-periodic probability density functions on $[-\pi, \pi]$ and demonstrate inversion formula (36) developed in corollary 4 for $\alpha > -1$.

Consider the following functions in $L^1_{w,\alpha}(\mathbb{R}_+) \cap L^2(\mathbb{R}_+)$ as well as their 2-sine transform $T_2 f$:

Example 1.

(a) $f_1(x) = \mathrm{e}^{-x^2}$, $T_2 f_1(y) = \frac{\sqrt{\pi}}{4}\left(1 - \mathrm{e}^{-y^2}\right)$.

(b) $f_2(x) = x^2 \mathrm{e}^{-|x|}$, $T_2 f_2(y) = \frac{8y^2(3+6y^2+8y^4)}{(1+4y^2)^3}$.

(c) $f_3(x) = \frac{1}{(1+x^2)^2}$, $T_2 f_3(y) = \frac{\pi}{8}\left(1 - \mathrm{e}^{-2|y|}(1 + 2|y|)\right)$.

For $\alpha \neq 0, 2, 4, \ldots$, the transform $T_\alpha f$ is in general not explicitly given, though its graph remains fairly similar, see figure 1.

6.1. Direct approach

In application, one has to keep the following two issues with the direct approach in mind. The operator $\mathcal{G}^{-1}$ defined in corollary 1 only fulfills injectivity, but it is not surjective. Secondly, $\mathcal{G}^{-1}$ is in general not a continuous operator. Therefore a straightforward application of $\mathcal{G}^{-1}$ does not automatically yield f. The reason for the above-mentioned arises from the fact that $\inf_{x>0} \mu(x) = 0$, where μ was defined in equation (12). Hence, the function $1/\mu$ is not bounded and multiplication by this function does not define a linear bounded operator on $L^2\left(\mathbb{R}_+, \frac{\mathrm{d}x}{x}\right)$. To deal with this we approximate $1/\mu$ by

$$\frac{1}{\mu}\mathbb{1}_{\{|\mu|>\varepsilon\}}$$

for some small $\varepsilon > 0$, and estimate the function f by

$$\tilde{f}(x) = \left(\mathcal{M}^{-1}\mathcal{F}_+^{-1}\frac{1}{\mu}\mathbb{1}_{\{|\mu|>\varepsilon\}}\mathcal{F}_+\mathcal{M}\left[z^{-1}g\left(z^{-1}\right)\right]\right)(x). \tag{38}$$

To simplify the numerical implementation, note that for any function $u \in L^2\left(\mathbb{R}_+, x^c\, \mathrm{d}x\right)$

$$\begin{aligned}\mathcal{F}_+u(x) &= \int_{\mathbb{R}_+} \mathcal{M}u(y)\mathrm{e}^{-\mathrm{i}\log(x)\log(y)}\frac{\mathrm{d}y}{y}\\ &= \int_{\mathbb{R}_+} y^{\frac{c+1}{2}}u(y)\mathrm{e}^{-\mathrm{i}\log(x)\log(y)}\frac{\mathrm{d}y}{y} = \int_{\mathbb{R}_+} y^{\frac{c-1}{2}-\mathrm{i}\log(x)}u(y)\mathrm{d}y.\end{aligned}$$

Thus, we define $\mathcal{H} : L^2\left(\mathbb{R}_+, x^c\, \mathrm{d}x\right) \to L^2\left(\mathbb{R}_+, \frac{\mathrm{d}x}{x}\right)$ by

$$\begin{aligned}\mathcal{H}g(x) &= \mathcal{F}_+\left[y^{-1}g\left(y^{-1}\right)\right](x) = \int_{\mathbb{R}_+} y^{\frac{c-1}{2}-\mathrm{i}\,\log(x)}y^{-1}g\left(y^{-1}\right)\mathrm{d}y\\ &= \int_{\mathbb{R}_+} y^{\frac{c-3}{2}-\mathrm{i}\,\log(x)}g\left(y^{-1}\right)\mathrm{d}y.\end{aligned}$$

Similarly, we introduce $\mathcal{H}_2 : L^2\left(\mathbb{R}_+, x^c\, \mathrm{d}x\right) \to, L^2\left(\mathbb{R}_+, \frac{\mathrm{d}x}{x}\right)$ by

$$\begin{aligned}\mathcal{H}_2w(z) &= \mathcal{M}^{-1}\mathcal{F}_+^{-1}w(z) = z^{-\frac{c+1}{2}}\mathcal{F}_+^{-1}w(z)\\ &= z^{-\frac{c+1}{2}}\frac{1}{2\pi}\int_{\mathbb{R}_+} w(x)\mathrm{e}^{\mathrm{i}\log(x)\log(z)}\frac{\mathrm{d}x}{x}\\ &= \frac{z^{-\frac{c+1}{2}}}{2\pi}\int_{\mathbb{R}_+} w(x)x^{\mathrm{i}\,\log(z)-1}\mathrm{d}x.\end{aligned}$$

Then $\tilde{f}$ is computed by

$$\tilde{f}(x) = \left(\mathcal{H}_2\frac{1}{\mu}\mathbb{1}_{\{|\mu|>\varepsilon\}}\mathcal{H}g\right)(x). \tag{39}$$

Recall that the constant $c = 1 + \delta$, where $\delta > 0$ such that $\alpha \geqslant 1 + \delta/2$, thus $1 < c \leqslant 2\alpha - 1$. Furthermore, the constant c directly affects the decay of the integrand in the definition of μ, i.e. the larger c the faster its decay. We therefore set c as large as possible, that is $c = 2\alpha - 1$, in the case $0 < \alpha < 2$. In the case $\alpha > 2$, values of $c > 3$, and thus the exponent $(c - 3)/2 > 0$ in the operator $\mathcal{H}$ above lead to difficulties during numerical integration. It proves to be more convenient to set $c = 3 \in (1, 2\alpha - 1]$ here.

The functions f_1 and f_2 of example 1 are contained in the space $L^2(\mathbb{R}_+, x^c\, \mathrm{d}x)$ for all $\alpha > 1$, hence the inversion formula from corollary 1 is applicable for all $\alpha > 1$. On the other hand, function f_3 fulfills this condition only for $\alpha \in (1, 2]$. The results for all three example functions in the case $\alpha = 2$ are displayed in figure 2. The inversion was performed with $\varepsilon = 0.025$.

The choice of ε is crucial for the precision of the inversion. The closer ε is to 0, the better the results of the inversion, but computation takes a significantly larger amount of time. Allowing
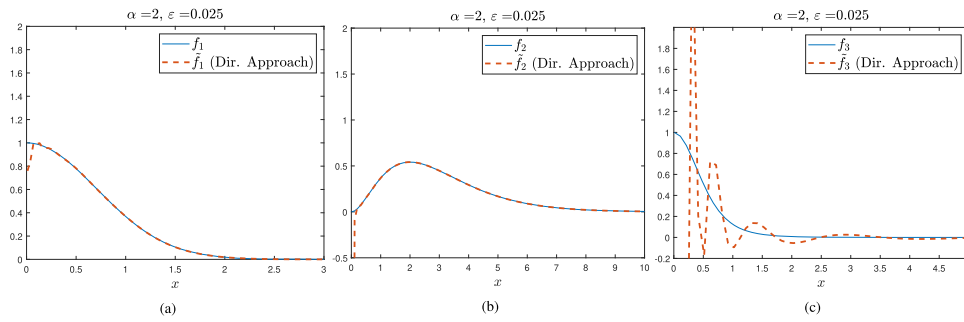
Figure 2. Direct approach, $\alpha = 2$. Inversion performed with $\varepsilon = 0.025$. Solid blue line shows the actual functions f_1, f_2, f_3. The dashed red line shows the result of the inversion of the direct approach.
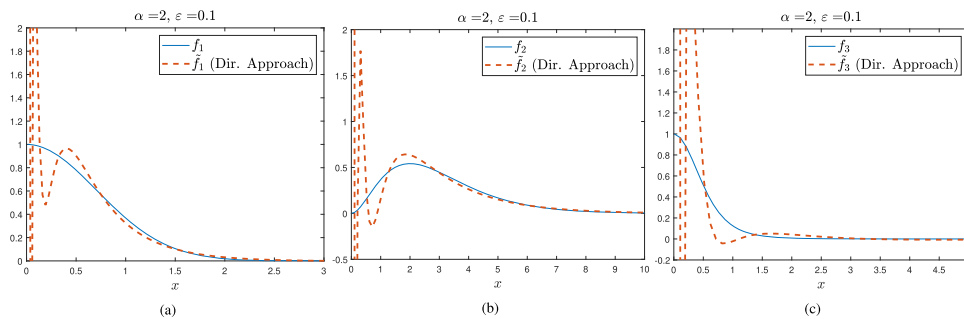

Figure 3. Direct approach, $\alpha = 2$. Inversion performed with $\varepsilon = 0.1$ for all three examples. Solid blue line shows the actual functions f_1, f_2, f_3. The dashed red line shows the result of the inversion of the direct approach.

for a larger ε reduces computation time, but large deviations from the expected result can be seen in figure 3, where the inversion was performed for all three example functions with $\varepsilon = 0.1$. Moreover, the inversion for the functions f_1 and f_2 is significantly faster than in the case of f_3.

In the following, only example f_2 is considered. The inversion is computed for the cases $\alpha \in \{10, 3, 1.5\}$. The results are illustrated in figure 4. Numerical computation takes a significantly larger amount of time for smaller α, but at the same time a larger choice ε suffices.

The inversion hinges on the behavior of the function μ which directly depends on α. Figure 5 depicts the function $|\mu|$ on the left-hand side as well as the real part of $1/\mu(x)\mathbb{1}_{\{|\mu(x)|>0.1\}}$ on the right-hand side for various values of α with $c = 2\alpha - 1$ (or $c = 3$ for $\alpha \geqslant 2$). The larger α the faster and less fluctuating the decay of $|\mu|$. Thus, the function $1/\mu(x)\mathbb{1}_{\{|\mu(x)|>0.1\}}$ cuts off sooner to 0 which directly contributes to computation of the integral operator $\mathcal{F}_+^{-1}$ in equation (38). Additionally, figure 5 emphasizes how choosing ε too small when dealing with smaller α is counterproductive, for example consider the case $\alpha = 1.25$. The corresponding dotted line on the left-hand side of figure 5 is fluctuating, and $|\mu|$ fails to fall below $\varepsilon = 0.1$. Thus, $1/\mu(x)\mathbb{1}_{\{|\mu(x)|>0.1\}}$ on the right-hand side of the plot is also fluctuating a lot and does not cut off to 0 as in the other cases. This will lead to difficulties during numerical integration and prolonged computation times.
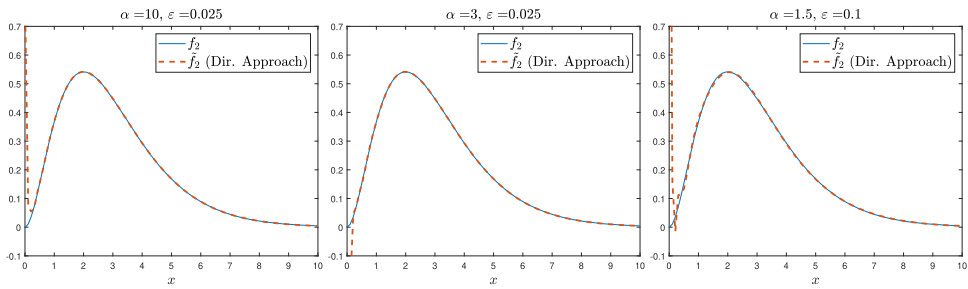
Figure 4. Direct approach, $\alpha \in \{10, 3, 1.5\}$. Inversion performed for f_2. Solid blue line shows the actual function f_2. The dashed red line shows the result of the inversion of the direct approach.
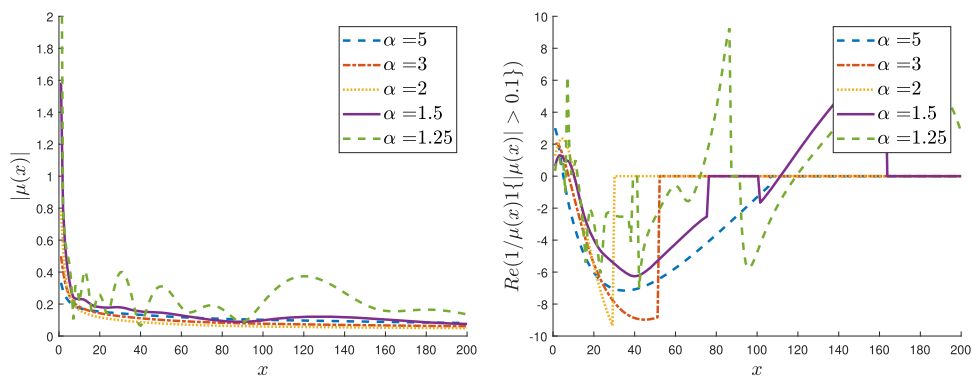

Figure 5. The functions $|\mu(x)|$ (left) and $1/\mu(x)\mathbb{1}_{\{|\mu(x)|>0.1\}}$ (right) for different values of α with $c = 2\alpha - 1$ ($c = 3$ for $\alpha \geqslant 2$).

On another note, for $\alpha \neq 2$ the function $g = T_\alpha f$ is not given in a closed formula which makes applications of integral transforms to it numerically challenging, as the inversion formula (38) essentially involves threefold integration, i.e. by T_α itself and by $\mathcal{F}_+, \mathcal{F}_+^{-1}$, respectively. Therefore, the function g was sampled discretely on the interval $[0, 20]$ with a step size of 10^{-6} between each sample point. Linear interpolation and constant extrapolation with the last sample point was used as an estimate for g. The upper bound of the interval was chosen such that g is approximately constant beyond that point.

6.2. Fourier approximation approach

We consider the functions given in example 1. Function values of the Fourier transform of the wanted function f are the solution of the system of linear equations $\boldsymbol{\eta} = \boldsymbol{C} \cdot \boldsymbol{\xi}$ described in section 4.2. Recall, the vectors $\boldsymbol{\xi} \in R^N$ containing function values of the Fourier transform, $\xi_n = \hat{f}_R\left(n\frac{R}{N}\right)$, and $\boldsymbol{\eta} \in R^N$ given by $\eta_n = T_\alpha f\left(n\frac{R}{2N}\right) - \frac{c_0}{2}\mathcal{F}f(0)$ for $n = 1, \ldots, N$, as well as the matrix $\boldsymbol{C}$ defined in proposition 1.

The integer R should be chosen as large as possible. Under the assumption that the Fourier transform $\mathcal{F}f$ is negligibly outside of the interval $[-R, R]$, we choose R large enough such that $T_\alpha f(y)$ is approximately constant for all $y > R$. Furthermore, note that $T_\alpha f(y) \approx \frac{c_0}{2}\mathcal{F}f(0)$ for
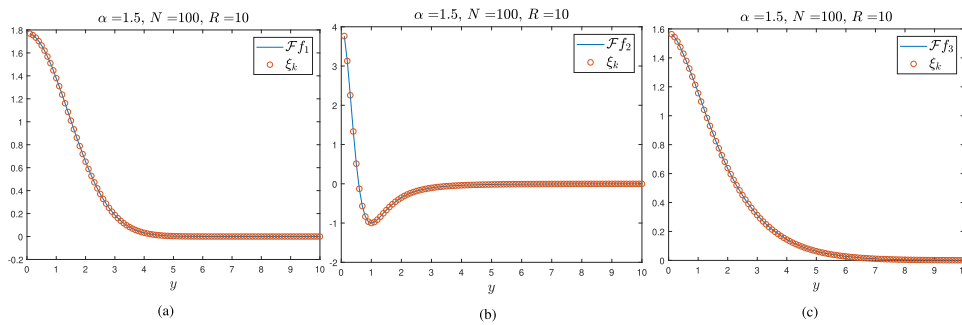
Figure 6. System of linear equations, $\alpha = 1.5, N = 100, R = 10$. Solid blue line shows the Fourier transform of the examples f_1, f_2 and f_3. The red circles are the solution of the system of linear equations $\boldsymbol{\xi}$.

large $y > R$. Hence, we chose $\mathcal{F}f(0) \approx 2T_\alpha f(y)/c_0$ for some large $y > R$. Lastly, the larger N the better in general, as this will make for finer sampling.

Figure 6 shows the solution $\boldsymbol{\xi}$ of the system of linear equations for all three examples and the case $\alpha = 1.5$ with $N = 100$ and $R = 10$.

On the other hand, when fixing α and N, choosing R too small is directly reflected in the results for $\boldsymbol{\xi}$, which is to be expected. For example choosing $R = 1$ would imply the assumption that $\mathcal{F}f$ vanishes outside of the interval $[-1, 1]$, which cannot be true as the function $T_\alpha f(y)$ is still increasing for $y > 1$ in all three examples f_1, f_2, f_3, see figure 1(a).

Contrary to that, larger R also show good results for $\boldsymbol{\xi}$. But since the number of sample points is fixed with N, the larger R the coarser the grid on which the Fourier transform $\mathcal{F}f$ is determined, which will effect the precision of the interpolation to follow.

The sampling theory of Shannon as discussed before gives another useful interpolation method for the Fourier transform of the spectral density. By symmetry of the Fourier transform and choosing $\hat{f}(0) = \mathcal{F}f(0) \approx 2T_\alpha f(y)/c_0$ for some large $y > R$, the function values $\hat{f}_R(kR/N)$, $k = -N, \ldots, N$ are approximated by the solution of the system of equations $\boldsymbol{\xi}$. Using the truncated cardinal series defined in (27) we interpolate $\hat{f}_R$.

By comparison of $\hat{f}(n/(2B)) = \hat{f}(nR/N)$, the Nyquist rate $2B$ corresponds to the ratio N/R. Since we generally cannot assume f to be compactly supported, the convergence results previously stated, suggest that the ratio N/R should tend to infinity. In practice, we therefore choose R just like in the case of the linear interpolation large enough such that $T_\alpha f(y)$ is approximately constant for $y > R$. The integer N is then set as large as possible. We compute the estimate for the spectral density f by

$$f_R^{(N)}(x) = \frac{R}{2\pi N} \operatorname{rect}\left(\frac{xR}{2\pi N}\right) \sum_{n=-N}^{N} \hat{f}\left(n\frac{R}{N}\right) e^{-ixnR/N},$$

see theorem 4. Figure 7 shows the result of the inversion with $N = 100, R = 10$ (based on the results depicted in figure 6) for all three examples in the case $\alpha = 1.5$.

We performed the inversion with various values of $\alpha > 0$ for all three functions f_1, f_2 and f_3. With a suitable choice of N, R, different values of α seem to have no effect on the computation of $\boldsymbol{\xi}$. Figure 8 highlights the result for f_1 with $N = 100, R = 10$ and $\alpha = 10$.
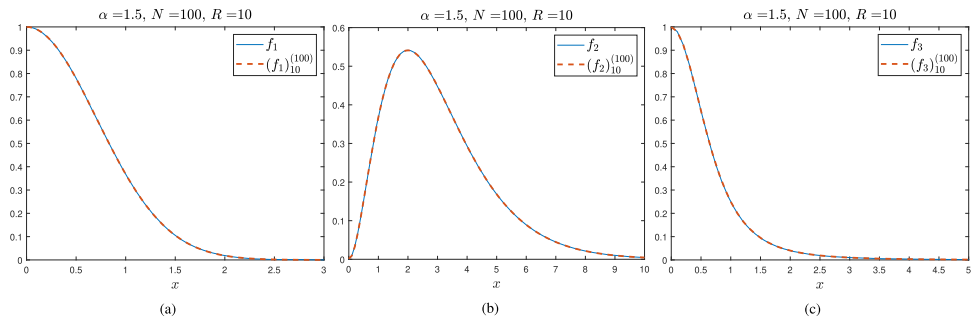
Figure 7. Band-limited interpolation, inversion, $\alpha = 1.5, N = 100, R = 10$. Solid blue line shows the functions f_1, f_2 and f_3. The dashed red line shows the inversion results.
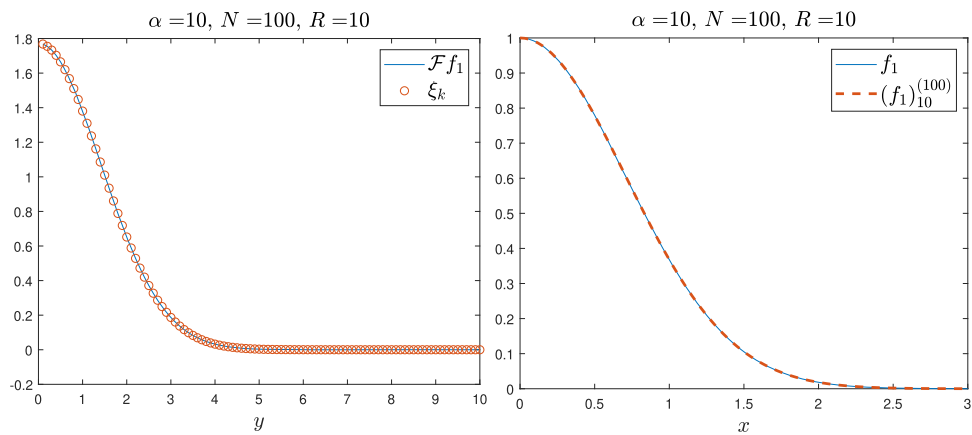

Figure 8. Band-limited interpolation, inversion, $\alpha = 10, N = 100, R = 10$. Approximation of the Fourier transform $\mathcal{F}f_1$ (left), and the inversion results (right).

Remark 6. In remark 3 the possibility of linear interpolation was mentioned. Our numerical experiments show that there seemed to be no visible difference in the results of either interpolation method. Linear interpolations performs slightly faster but is on the other hand also marginally less accurate. See table 1 for a comparison between all methods for example f_2.

6.2.1. Smoothing. Section 4.4 touched upon the topic of noise contamination of the function $T_\alpha f$. To simulate this scenario, we artificially added noise to the function $T_\alpha f$. For all three functions f_1, f_2 and f_3, their transform $T_\alpha f$ is sampled on the interval $[0, 20]$ at 400 equidistant points. We then added Gaussian noise with a standard deviation of 0.1 to each sample point, see figure 9.

Recall from section 4.4, that we compute the smoothed solution of the function f by $f_{R,\gamma}^{(N)} = \mathcal{F}^{-1}\left(f_R^{(N)} \cdot \psi_\gamma\right)$, where ψ_γ is the reconstruction kernel with smoothing parameter $\gamma > 0$ satisfying $\psi_\gamma = \mathcal{F}e_\gamma$ for a given mollifier function e_γ, and $f_{R,\gamma}^{(N)}$ is the approximation of the Fourier transform $\mathcal{F}f$ as computed in the previous sections.

There are many options for mollifiers available. We consider the following two examples of mollifiers $e^{(1)}, e^{(2)}$ and their corresponding reconstruction kernels $\psi^{(1)}, \psi^{(2)}$.

Table 1. Comparison between the direct approach and the Fourier approximation method (with band-limited or linear interpolation). Computations were performed for f_2 (cf example 1(b)) with $R = 10$, $N = 100$. The computation time was measured for the computation of the approximate $\hat{f}_2$ at 100 equidistantly spaced points on $[0, R]$.

Method	$\alpha = 2$		$\alpha = 1.5$	
	Computation time (in sec.)	L^2-distance to f_2 on $[0, R]$	Computation time (in sec.)	L^2-distance to f_2 on $[0, R]$
Direct approach[a]	386.8818	4.7530×10^{-2}[b]	1.0711×10^5	0.5048[c]
Fourier Band-limited	1.2031	5.4255×10^{-4}	1.5785	5.4383×10^{-4}
approximation Linear interp.	0.0469	7.3239×10^{-3}	0.4423	7.3239×10^{-3}

[a]For $\alpha = 2$ we used $\varepsilon = 0.025$ and the analytical form of $T_2 f_2$ given in example 1(b). For $\alpha = 1.5$ we set $\varepsilon = 0.1$ and used a discrete sample of $T_{1.5} f_2$ with a sample step size of 10^{-6}.
[b]Computation was performed on $[0.05, R]$ only as computation times increase tremendously the closer the left integration boundary is to 0. The error becomes larger, too.
[c]Due to high computation times, we used the built-in trapezoid discretization for numerical integration.
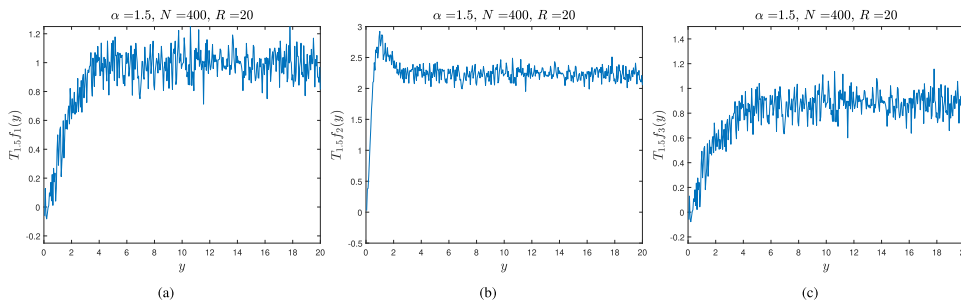

Figure 9. Noisy data. Gaussian noise added to $T_{1.5}f$, sampled on the interval $[0, 20]$ at 400 equidistant points, for all three spectral densities f_1, f_2 and f_3.

Example 2.

(a) $e^{(1)}(x) = \begin{cases} 1 - |x| & , -1 \leqslant x \leqslant 1, \\ 0 & , \text{ else,} \end{cases}$ with $\psi^{(1)}(y) = 2\left(1 - \cos(y)\right)/y^2$, $y \in \mathbb{R}$.

(b) $e^{(2)}(x) = e^{-\pi x^2}$, $x \in \mathbb{R}$,   with $\psi^{(2)}(y) = e^{-y^2/(4\pi)}$, $y \in \mathbb{R}$.

The solution $\boldsymbol{\xi}$ of the linear equation $\boldsymbol{\eta} = \boldsymbol{C}\boldsymbol{\xi}$ is interpolated linearly as well as with the truncated cardinal series, see figure 10. Whichever interpolation method is employed before does not play a significant role. The smoothed solution is computed for all three examples with $\gamma = 0.5$. Smoothing was performed with reconstruction kernel $\psi^{(1)}$. The results are displayed in figure 11.

6.2.2. The case $-1 < \alpha < 0$. In the following we consider negative values $-1 < \alpha < 0$. Figure 12 shows the respective transforms for the functions of example 1. The transform $T_\alpha f$ is not defined at 0, and as the parameter α approaches -1 the irregularities in the graph of $T_\alpha f$ become more sizable, which is explained by the increasing difficulty regarding the integrability of the integral kernel $|\sin(t/2)|^\alpha$.
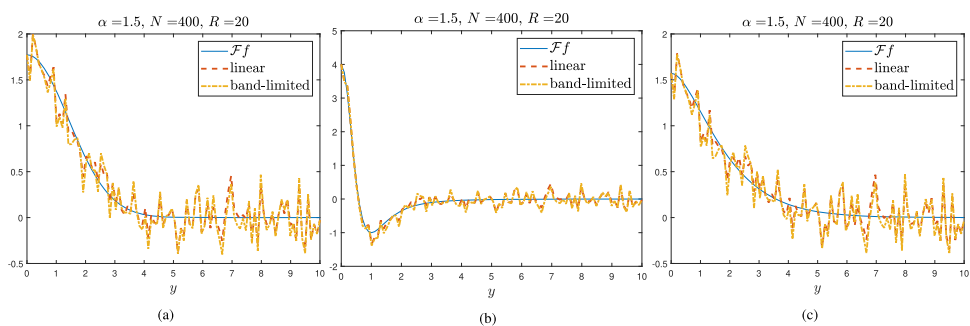
Figure 10. Noisy data. Linear interpolation and band-limited interpolation in the case $\alpha = 1.5$ for all three example functions.
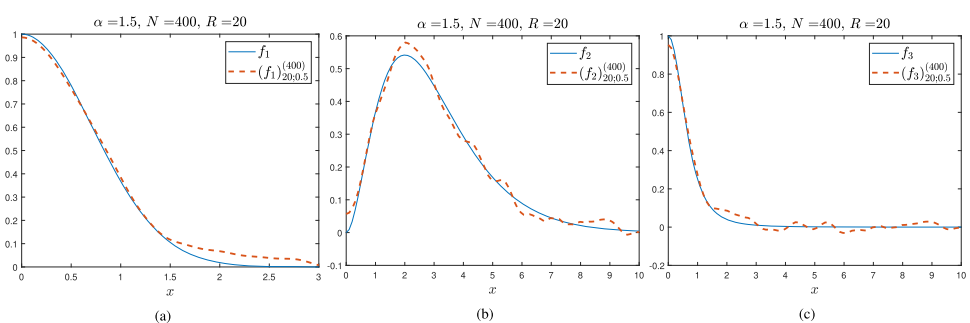

Figure 11. Smoothed, band-limited interpolation, inversion. Smoothed solution for the case $\alpha = 1.5$. Inversion performed with $N = 400, R = 20$ and reconstruction kernel $\psi_{0.5}^{(1)}$ with $\gamma = 0.5$.
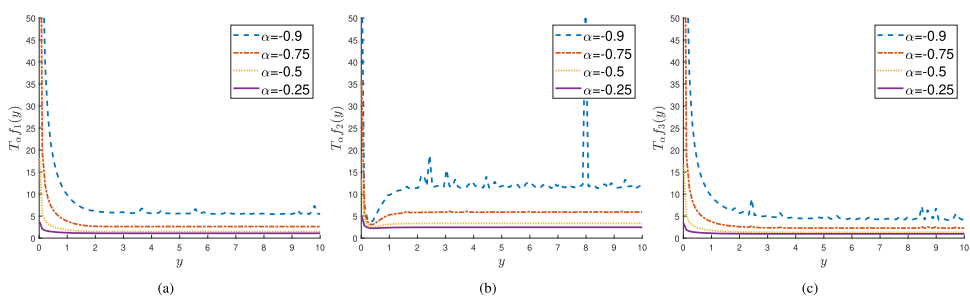

Figure 12. $\alpha \in (-1, 0)$. Plots of the function $T_\alpha f$ for all three examples f_1, f_2 and f_3 with $\alpha \in \{-0.9, -0.75, -0.5, -0.25\}$.

Figures 13 and 14 show the inversion results of all three examples using band-limited interpolation for $\alpha = -0.5$ as well as for example f_2 and $\alpha \in \{-0.9, -0.75, -0.25\}$, respectively. All results were computed with $N = 100, R = 10$. For the case $\alpha = -0.9$, the reconstruction
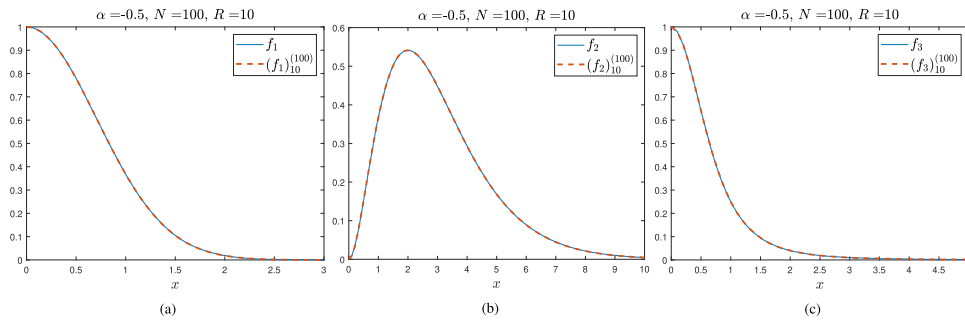
Figure 13. Band-limited interpolation, inversion, $\alpha = -0.5, N = 100, R = 10$. Solid blue line shows the functions f_1, f_2 and f_3. The dashed red line shows the inversion results.
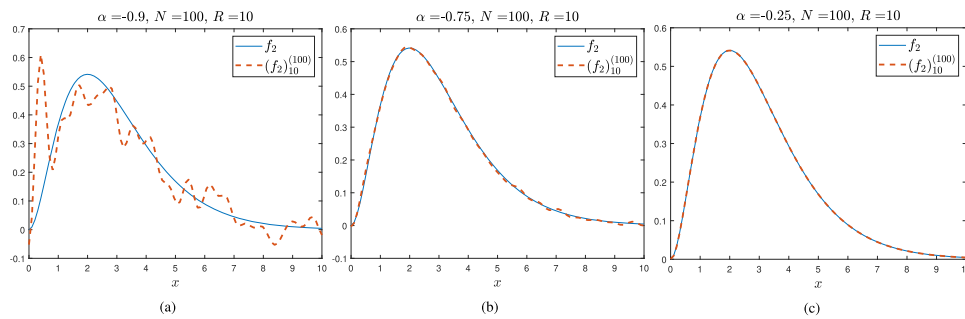

Figure 14. Band-limited interpolation, inversion, $\alpha \in \{-0.9, -0.75, -0.25\}, N = 100, R = 10$. Solid blue line shows the function f_2. The dashed red line shows the inversion results.

of f_2 shows larger deviations. This was to be expected looking at the irregularities of the transform $T_{-0.9} f_2$ in figure 12(b). For f_1 and f_2 the results for values of α close to -1 are better as the graphs of their transforms $T_{\alpha} f$ do not show such severe spikes.

6.3. Spherical α-cosine transform on S^1

We consider the following examples of even probability density functions on the unit circle S^1:

Example 3.

(a) $f_1(x) = |\sin(x - h)|/4$ with $h \in [-\pi, \pi]$.

(b) $f_2(x) = I^{-1} e^{\cos(4(x-h))}$ with $h \in [-\pi, \pi]$, where I is a normalizing constant.

(c) $f_3(x; \mu, \kappa) = M(1/2, 1, \kappa)^{-1} e^{\kappa \cos(x-\mu)^2}$ (*two-dimensional Watson distribution*), where the normalization factor $M(1/2, d/2, \kappa)$ is the d-dimensional Kummer function. Samples of this distribution concentrate around $\pm \mu \in [-\pi, \pi]$ with concentration parameter $\kappa > 0$.

Their two-dimensional spherical α-cosine transform reads $K_{\alpha,S} f(y) = \int_{-\pi}^{\pi} |\cos(y - x)|^{\alpha} f(x) \mathrm{d}x$ for $\alpha > -1$. Applying corollary 4, we get an estimate f_N for the density function f
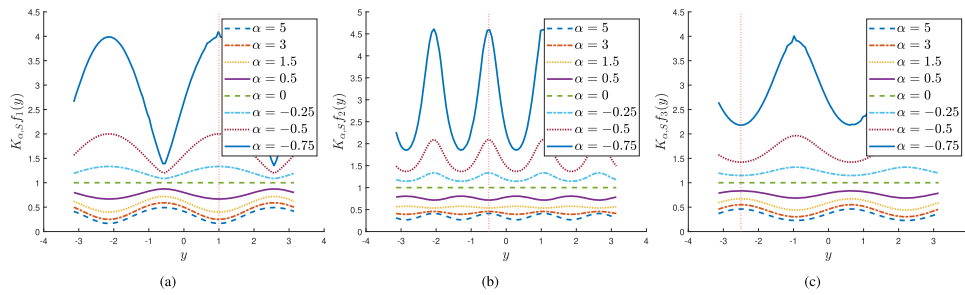
Figure 15. Spherical α-cosine transform on S^1. Plots of $R_\alpha f$ for the examples f_1 (with $h = 1$), f_2 ($h = -0.5$) and f_3 (with $\mu = -2.5$, $\kappa = 1$) and $\alpha \in \{5, 3, 1.5, 0.5, 0, -0.25, -0.5, -0.75\}$. The vertical red line illustrates the horizontal shift of the examples from their respective version which is even about 0.
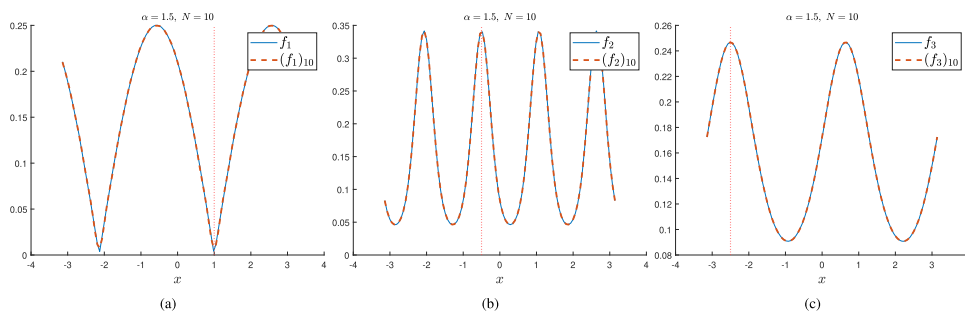

Figure 16. Spherical 1.5-cosine transform on S^1, inversion, $N = 10$. Inversion results for all three examples f_1, f_2 (with $h = 1$) and f_3 (with $\mu = -2.5$, $\kappa = 1$). The solid blue line shows the actual function f. The red dashed line shows the result of the inversion.

given by

$$f_N(x) = \frac{1}{2\pi} \left(1 + \sum_{n=-N,\ n\neq 0}^{N} \frac{\widehat{K_{\alpha,s}f}(2n)}{\tilde{c}_n} e^{i2nx} \right).$$

Figure 15 shows the spherical α-cosine transform of all three densities f_1, f_2, f_3 from example 3 with various values of $\alpha > -1$. The results of the reconstruction of all three functions from their Fourier coefficients for $\alpha = 1.5$, using corollary 4, are given in figure 16. The results inversion results for other values of $\alpha > -1$ show an identical picture to figure 16, and thus are omitted here.

7. Discussion

Corollary 1 gives an inversion operator of T_α that is injective on the space of square integrable functions on the real positives with respect to a weighted Lebesgue measure. The direct approach provides a direct computational formula for the function f from its α-sine transform $T_\alpha f$, and generally works on a larger class of transformations than the presented α-sine transform, but is lacking in terms of efficiency. The practical implementation of the underlying

theory quickly proves to be quite cumbersome. The numerical instability of the function μ_+ as well as the Fourier transformation $\mathcal{F}_+$ on the multiplicative group $(\mathbb{R}_+, \cdot)$ require tremendous computational effort. Most importantly, the direct approach is only applicable for $\alpha > 1$.

The choice of the cut-off parameter ε significantly impacts the results of the inversion. An insufficiently small choice leads to large deviations around 0. Very small ε reduce these deviations but at the price of very long computation times. Satisfying results could only be achieved when accepting several hours of computation (on a modern Intel i5 8500 6-core CPU). In our examples, $T_\alpha f$ needed to be sampled and an interpolation was used as an approximate. A direct application of corollary 1 to the integral form of $T_\alpha f$ led to no results as numerical integration failed. The step size of the sample had to be chosen as small as 10^{-6}. Larger step sizes increased computation times enormously or ended in diverging numerical integration. See table 1 for a comparison of the direct approach to the Fourier approximation approach in terms of computation time and accuracy.

The Fourier approximation approach is based on the series representation of $T_\alpha f$ given in theorem 2, which holds for all $\alpha > -1$. The specific Fourier expansion of the integral kernels $|\sin(x)|^\alpha$ and $|\cos(x)|^\alpha$, respectively, allow for the construction of a fast and efficient approximative inversion method. In the case $\alpha = 2$, the transform $T_2 f$ is simply a linear transformation of the Fourier transform $\mathcal{F}f$, thus inversion is achieved by a simple application of the inverse Fourier transform. In any other case $\alpha > -1$, the representation of $T_\alpha f$ as a series of the Fourier transform $\mathcal{F}f$, and the resulting system of linear equation from proposition 1 enable us to compute an approximate of $\mathcal{F}f$ efficiently. Applying the inverse Fourier transform allows us to estimate the function f.

The presented Fourier approximation method is fast and delivers accurate results for the inversion in a matter of seconds. The solution of the system of linear equations involved is easily computed since the matrix C is triangular and non-singular by construction. We have seen that the parameters N and R can be chosen in a practical manner. Our computations were performed with only $N = 100$ equidistant samples of Tf on the interval $[0, 10]$. This is a huge advantage over the direct approach, where only a much smaller step size of 10^{-6} led to acceptable results.

Table 1 compares the numerical performance of all methods for the function f_2 from example 1(b). Linear interpolation performed slightly faster than band-limited interpolation but is less accurate, and both perform tremendously faster and are more accurate than the direct approach. Most of the error in the direct approach stems from the fluctuation of the inversion near 0, e.g. on the interval $[0.5, R]$ the L^2-distance is much smaller. Still the long computation times are an immense drawback. But most importantly, the advantage of the Fourier approximation approach lies in its applicability for all $\alpha > -1$.

When dealing with noise inflicted input data, the convolution property of the Fourier transformation enables us to compute a smoothed solution to our inversion problem. Multiplication of the interpolated approximate of the Fourier transform of f with a reconstruction kernel corresponds to the convolution of f with the corresponding mollifier. For our synthetically generated, noise corrupted data, satisfactory smoothed solutions are still achieved when dealing with noise that is considerably higher than the examples shown in section 6.2.1.

The closer α gets to -1, the more difficult it is to compute satisfactory inversion results, as we have seen in the case $\alpha = -0.9$ for example f_2. The deviation of the inversion from its target is deeply connected to the numerical integrability of the integral kernel for α close to -1. Signs of the numerical instability can be seen immediately from the spikes in the transform $T_\alpha f$. A viable solution to this can be achieved by smoothing $T_\alpha f$ as we have done in our sample with synthetically noise inflicted data before.

Lastly, we also derived a series representation for the two-dimensional spherical α-sine and cosine transforms with the identical coefficients as for the transforms on $\mathbb{R}_+$. This allows us establish an inversion algorithm which computes the Fourier coefficients of an even function on the unit circle from the Fourier coefficients of its two-dimensional spherical transform. For $\alpha > -1$, $\alpha \neq 0, 2, 4, \ldots$ successful inversion results for probability density functions on the unit circle S^1 are achieved.

Data availability statement

No new data were created or analysed in this study.

ORCID iDs

Ly Viet Hoang ⬤ https://orcid.org/0000-0001-5592-7979

References

[1] Bailey W N 1964 *Generalized Hypergeometric Series* (New York: Stechert-Hafner)
[2] Bateman H 1981 *Higher Transcendental Functions* vol 1 (New York: McGraw-Hill)
[3] Bracewell R N 2002 *The Fourier Transform and its Applications* (New York: McGraw-Hill)
[4] Brown J L 1967 On the error in reconstructing a non-bandlimited function by means of the bandpass sampling theorem *J. Math. Anal. Appl.* **18** 75–84
[5] Folland G B 1992 *Fourier Analysis and its Applications* (Pacific Grove: Wadsworth & Brooks/Cole)
[6] Glück J, Roth S and Spodarev E 2019 A solution to a linear integral equation with an application to statistics of infinitely divisible moving averages (arXiv:1807.02003)
[7] Goodey P and Howard R 1990 Processes of flats induced by higher dimensional processes *Adv. Math.* **80** 92–109
[8] Goodey P and Weil W 1992 Centrally symmetric convex bodies and the spherical Radon transform *J. Differ. Geom.* **35** 675–88
[9] Goodey P and Weil W 1993 Zonoids and generalizations *Handbook of Convex Geometry* ed Gruber and Wills (Amsterdam: North-Holland)
[10] Grafakos L 2014 *Classical Fourier Analysis* (*Springer Graduate Texts in Mathematics* vol 249) (New York: Springer)
[11] Groemer H 1996 *Geometric Applications of Fourier Series and Spherical Harmonics* (Cambridge: Cambridge University Press)
[12] Helgason S 1984 *Groups and Geometric Analysis: Integral Geometry, Invariant Differential Operators, and Spherical Functions* (Orlando: Academic)
[13] Kolmogorov A N and Fomin S V 1975 *Reelle Funktionen und Funktionalanalysis* (Berlin: Deutscher Verlag der Wissenschaften)
[14] Marks R J 1991 *Introduction to Shannon Sampling and Interpolation Theory* (Berlin: Springer)
[15] Matheron G 1975 *Random Sets and Integral Geometry* (New York: Wiley)
[16] Mecke J 1981 Formulas for stationary planar fibre processes III—intersections with fibre systems *Math. Oper.forsch. Stat. Ser. Stat.* **12** 201–10
[17] Quarteroni A, Sacco R and Saleri F 2007 *Numerical Mathematics* (Berlin: Springer)
[18] Rahman Q I and Vértesi P 1992 On the L^p convergence of Lagrange interpolating entire functions of exponential type *J. Approx. Theory* **69** 302–17
[19] Rubin B 2002 Inversion formulas for the spherical Radon transform and the generalized cosine transform *Adv. Appl. Math.* **29** 471–97
[20] Rubin B 2008 Intersection bodies and generalized cosine transforms *Adv. Math.* **218** 696–727
[21] Samorodnitsky G and Taqqu M S 1994 *Stable Non-Gaussian Random Processes: Stochastic Models with Infinite Variance* (London: Chapman and Hall)
[22] Schmeisser H J and Sickel W 2000 Sampling theory and function spaces *Appl. Math. Rev.* **1** 205–84

[23] Spodarev E 2001 On the rose of intersections of stationary flat processes *Adv. Appl. Probab.* **33** 584–99

[24] Weil W 1976 Centrally symmetric convex bodies and distributions *Isr. J. Math.* **24** 352–67

[25] Zayed A I 1993 *Advances in Shannon's Sampling Theory* (Boca Raton, FL: CRC Press)